Oxidative bromination and oxidation of organic substrates catalyzed by bis[2,2'-hydroxyphenylbenzimidazole]Fe(III) complex entrapped in zeolite-Y cavity

Shilpa. E. R, Gayathri. V*

*Department of Chemistry, Bangalore University, Central college campus, Dr. Ambedkar Veedi, Bangalore-560001, Karnataka, India.

*Corresponding author email: gayathritvr@yahoo.co.in, Phone: 080-22961348

Abstract

BACK GROUND: Zeolite encapsulated transition metal complexes have proven to be better catalysts for most of the organic transformations as they share advantages of both homogeneous and heterogeneous catalysts because the complex inside the zeolite cage could move within the cavity at the same time cannot come out of it owing to its size. Hence, various reports claim the application of these encapsulated complexes in various organic transformations. Introduction of bromine into aromatic compounds is an important-fundamental reaction in organic chemistry. On the other hand, oxidations of saturated and unsaturated compounds also find their application in synthesis of fine chemicals.

RESULTS: The peak positions in cyclic voltammogram of encapsulated complex were unaltered accompanied by increase in current with scan rates substantiating the encapsulation of the complex within the cavity. This complex was catalytically active in presence of H_2O_2 towards the oxidation of cyclohexane and ethylbenzene. Its catalytic efficiency was examined towards oxidative bromination of organic substrates using KBr at room temperature wherein high para-selectivity was obtained. It displayed better conversion/selectivity than $Fe(opbmzl)_2NO_3$ retaining its catalytic activity up to 5 consecutive runs. Plausible mechanisms involving hydro-peroxo intermediate have been proposed.

This article has been accepted for publication and undergone full peer review but has not been through the copyediting, typesetting, pagination and proofreading process, which may lead to differences between this version and the Version of Record. Please cite this article as doi: 10.1002/jctb.5201

CONCLUSION: Zeolite encapsulated Bis[2,2'-hydroxyphenylbenzimidazole]Fe(III) complex behaved as a versatile catalyst for various organic transformations.

Key words: Iron hydro-peroxo intermediate; oxidative bromination; electrochemical studies; heterogeneous catalysis, zeolite.

1.0 Introduction

Encapsulation of transition metal complexes within the voids of zeolite coalesce the reactivity of the metal complex with the sturdiness and stereochemistry of zeolite host. [1] It also affords an expedient path for heterogenization of homogeneous complexes that could be applied in catalysis and gas purification. [2-3] These catalysts proffer the advantage of shape selectivity and site isolation, due to the zeolite matrix, while retaining the solution reactivity of the metal complex. It has been widely recognized that space constraints imposed by the zeolite as well as specific interactions with the zeolite framework can persuade structural and functional modifications of the complex as compared to its solution that manifests its reactivity and catalytic properties. [4-7] Oxidative bromination is a process which generates electrophilic bromine using various oxidants. It has drawn the attention of researchers in recent years, as the organic bromides are widely used as synthetic precursors for various coupling reactions in organic and pharmaceutical synthesis beside their biological applications. [8] In the laboratory as well as industrial scale, however, bromination is generally carried out with hazardous, toxic and corrosive molecular bromine mostly in combination with chlorinated solvents. Moreover the use of molecular bromine causes a serious peril to the environment and human health due to its toxicity and corroding character and only one bromine atom is consumed in the reaction while the other is converted to HBr which escapes into the environment. [9] There are some reagents that have been developed as a substitute for Br_2, such as N-bromosuccinimide/1-butyl-3-

methylimidazolium bromide, $ZrBr_4$/diazene, $[K^+18\text{-crown-6}]Br_3$, 1-butyl-3- methylpyridinium tribromide, 3-methylimidazolium tribromide, 1-butyl-3-methylimidazolium tribromide, pentylpyridinium tribromide, ethylene bis(N-methylimidazolium) ditribromide.[10-17] Some systems including bromine as a reagent have also been developed. Such as, Br_2/Ag_2SO_4, $Br_2/SbF_3/HF$, Br_2/SO_2Cl_2/Zeolite, Br_2/Zeolite, Br_2/H_2O_2, Br_2/H_2O_2/Layered Double Hydroxide-WO_4, Br_2/tetrabutylammonium peroxydisulphate etc. [18-24] Besides being expensive in nature they have meager recovery and recycling of spent reagent and disposal of large amounts of HBr waste. Preparations of all these reagents involve liquid bromine at some stage, thereby, increasing the cost of the end-product. All the above accounted methods suffer from using not easily available compounds and others use highly-corrosive or expensive reagents. Therefore, catalytic oxidative bromination reaction has been still attracting attention to develop the more efficient method suitable for synthesis.

From green chemistry point of view, hydrogen peroxide is considered as the best oxidant for oxidative halogenation as the by-product obtained is only water. Aqueous H_2O_2 is capable of oxidizing bromide in absence of catalyst in highly acidic medium (pH < 3), whereas at pH > 5.0, it has to be activated by homogeneous or heterogeneous catalysts. This feature has provided impetus for the development of myriad useful catalysts or reagents including transition metals based systems for oxidative bromination by H_2O_2. [25-31]

Most of the model complexes reported were found to be catalytically active only in presence of acids. [32-34] These acids, although readily available and cheap, usually suffer from the drawbacks such as difficulty in separation from organic products and production of large volumes of hazardous wastes. [35-37] These disadvantages are of great concern in view of the growing ecological awareness in recent years. Though diverse materials have been explored as

catalysts for oxidative bromination, zeolite encapsulated transition metal complexes have been rarely used. [38-40] More over the application of Fe(III) complex encapsulated in zeolite-Y towards oxidative bromination is rarely studied.

Similarly, oxidations of aliphatic and aromatic alkanes are industrially important processes, as the resulting products find their applications in manufacture of textiles, fine chemicals and pharmaceuticals. At industrial level, these reactions are often carried out using stoichiometric quantity of reagents or under harsh conditions. In order to overcome these drawbacks, new catalytic materials have been designed that could be operated in mild conditions. [41-45]

Hence, present work is focused on synthesis and characterization of bis[2,2'-hydroxyphenylbenzimidazole]Fe(III) complex encapsulated in the cavity of zeolite-Y and investigation of its catalytic activity towards oxidative bromination of aromatics and oxidation of cyclohexane and ethylbenzene. Influence of external parameters on the catalytic activity of the encapsulated complex was investigated for better performance of the catalyst. Hence in this work, the encapsulated complex is used for oxidative bromination of few aromatic substrates.

2.0 Experimental

2.1 Chemicals and Reagents

Commercially available Na-Y zeolite was supplied from Sud-Chemie, India and was used as received without further purification. The other reagents like orthophenylenediamine, 4-aminophenol, nitrobenzene, anisole (S.d. fine chem. Ltd, India), diphosphorus pentoxide, orthophosphoric acid, 2,6-di-tert-butyl-4-methylphenol (BHT), salicylic acid, phenol, $Fe(NO_3)_3.9H_2O$, cyclohexane, aniline, toluene, ethylbenzene, benzene, silica gel, ethyl acetate, petroleum benzene, n-hexane (Merck), tetrabutylammonium bromide (Spectrochem. Pvt. Ltd,

India), vulcan carbon (Cabot corporation) and Methyl-1-phenyl-2-propanol (Sigma Aldrich) were used as received. 2-methyl-1-phenyl-2-propyl hydroperoxide (MPPH) was prepared according to a literature method using 2-methyl-1-phenyl-2-propanol.[46] All the solvents were purified prior to use.

2.2 Physical methods and analysis

All the samples were vacuum dried before analysis. The elemental analyses were obtained with an Elementar Vario micro cube CHNS analyzer. The iron content was determined using inductively coupled plasma-atomic emission spectroscopy (ICP-AES) at Atomic Mineral Directorate, Southern region, Bangalore. The surface area and pore volume were measured by Bruneur Emmett Teller (BET) method using Micromeritics surface area analyzer model ASAP 2020. The XRD patterns were recorded on a Panalytical X'pert Pro MPD powder X-ray diffractometer using Cu Kα radiation (λ = 1.542 Å) in the 2θ range 10 - 60˚ at a scanning rate of 0.25˚/min. The UV-visible-DRS spectra were measured using a Shimadzu UV-Vis-NIR model UV-3101P spectrophotometer having an integrating sphere attachment for the solid samples in $BaSO_4$. The IR spectra of the samples were recorded in the range 400-4000 cm^{-1} as KBr disks on a Shimadzu 8400 s FT-IR spectrometer. The ESR spectra were recorded using a Bruker EMX EPR spectrometer X-band, ν = 9.431GHz at room temperature (Indian Institute of Science, Bangalore). The electrochemical properties were studied by recording the cyclic voltammograms of $Fe(opbmzl)_2NO_3$ and encapsulated complexes on a EG & G Model Versastat IIA Galvanostat/ Potentiostat with a digital recorder by using 0.1 M tetrabutylammonium perchlorate (TBAP) as the supporting electrolyte in DMF. The working electrode was prepared by taking a 1:1 weight ratio of $Fe(opbmzl)_2NO_3$ or encapsulated metal complexes in 1 mL of milli Q water. This paste was coated on platinum flag of 8.0 cm^2 area; 2 mL of nafion binder (Sigma Aldrich) was then

added on this coating followed by air drying. The platinum flag electrode and standard calomel electrode (SCE) were used as the working and reference electrodes respectively. The CV of the $Fe(opbmzl)_2NO_3$ complex was taken both in solid and solution modes, using 0.01 M of the metal complex in DMF. Thermograms were recorded on a TA instrument under nitrogen atmosphere with heating rate of 10 °C/min from 20 to 1000 °C. The purity of the brominated products were confirmed from ^1H NMR spectral analyses using Bruker 400 MHz multinuclear NMR spectrometer at room temperature. All the reaction products were analyzed using a Shimadzu 14B gas chromatograph (GC) fitted with flame ionization detector using a BP-5 capillary column.

2.3 Synthesis

(a) Synthesis of Fe(III) exchanged zeolite-Y (Fe-Y)

In a typical experiment, 5 g of Na-Y zeolite was suspended in 300 mL distilled water containing $Fe(NO_3)_3.9H_2O$ (20.2 g, 50 mmol) and heated at 90 ˚C under stirring for 48 h. The obtained brown coloured solid was filtered, thoroughly washed with hot distilled water and then Soxhlet extracted using ethanol, till the filtrate was free from iron and subsequently dried at 150 ˚C for 12 h. The iron content in iron-exchanged zeolite-Y was found to be 1.7 %.

(b) Synthesis of zeolite encapsulated bis[2-(2'-hydroxyphenyl)benzimidazole]Fe(III) {$Fe(opbmzl)_2$-Y}

2-(2'-hydroxyphenyl)benzimidazole (ohpbmzl) and the $Fe(opbmzl)_2NO_3$ complex were synthesized according to the reported methods. [47-48]

$Fe(opbmzl)_2$-Y was synthesized by refluxing an ethanolic solution of ohpbmzl and Fe(III) exchanged zeolite-Y at 60 ˚C for 48 h and the product formed was washed with DMF and C_2H_5OH using Soxhlet extractor. The uncomplexed Fe(III) ions present in the zeolite-Y were

exchanged with Na^+ ions by treating with aqueous 0.1 M NaCl solution, filtered and washed with distilled water and dried at 120 ˚C for 24 h. Iron content in the encapsulated complex was determined by AAS and was found to be 0.45 % (Table 1)(Scheme 1).

(c) Catalytic activity towards probe reactions

(i) Oxidative bromination

Aqueous 30% H_2O_2 (2.27 g, 25 mmol) was added dropwise to the mixture of substrate (1.22 g, 10 mmol) and KBr (2.38 g, 11.0 mmol) taken in 10 mL of CH_3CN. 0.080 g of catalyst was added to it and the reaction mixture was stirred at room temperature. After the specified time of the reaction, the catalyst was filtered and solid was washed with ether. The combined filtrates were washed with saturated sodium bicarbonate solution. The organic extract was dried over anhydrous sodium sulfate and solvent was evaporated. The products were purified by column chromatography using ethyl acetate/petroleum benzene. The products were confirmed by ^1H NMR spectroscopic and gas chromatographic techniques.

(ii) Oxidation reactions

In a typical experiment, cyclohexane (5.1 g, 60 mmol) and aqueous 30% H_2O_2 (17.0 g, 150 mmol) were mixed in 10 mL CH_3CN and heated to 70 ºC. An appropriate amount of catalyst (0.120 g) was added and the reaction was carried out for 6 h. The reaction products were analyzed using GC at specific time intervals by withdrawing a small aliquot.

Ethylbenzene (4.2 g, 40 mmol), 30% aqueous H_2O_2 (9.06 g, 80 mmol) and catalyst (0.110 g) in 10 mL CH_3CN were heated at 60 ºC for 6 h. The reaction products were analyzed as mentioned in case of cyclohexane oxidation.

The effect of various parameters such as temperature, concentration of substrate and catalyst, substrate/H_2O_2 molar ratio and nature of solvents were checked to optimize the conditions for the best catalyst performance.

3.0 Results and discussion

3.1 X-ray diffraction studies

The XRD patterns of the NaY, Fe-Y, Fe(opbmzl)$_2$-Y and recycled Fe(opbmzl)$_2$-Y are presented in the Figure 1. The diffraction patterns of Fe-Y and Fe(opbmzl)$_2$-Y were similar to NaY but the relative intensity was drastically reduced. These observations specified that the zeolite framework did not undergo any significant structural changes during encapsulation. It was observed that the intensity of peaks due to (220) and (311) were reversed in case of Fe(opbmzl)$_2$-Y (220 < 311) as compared to that of NaY and Fe-Y (220 > 311) which could be due to displacement of cations in the cavity to other sites (I' and II) during the formation of complex in the cavity.[49-51]

In order to verify if the framework of Fe(opbmzl)$_2$-Y is altered or not, after its application in the probe reactions, its XRD pattern after recycling was examined and observed that there was no major changes in its framework.

3.2 Fourier Transform Infrared Spectral studies

The FT-IR spectrum of NaY displayed an intense broad band at 3509 cm^{-1} due to the presence of hydroxyl groups in the supercages and in the sodalite cages (Figure 2). [52] The bands below 1200 cm^{-1}, located at 580, 713-785 and 1020 cm^{-1} were attributed to the double ring, symmetric and asymmetric stretching of Al-O-Si framework vibrations, respectively. [53-54] The FT-IR spectrum of Fe(opbmzl)$_2$NO$_3$ complex exhibited peaks at 3143, 1608, 1298, 1474 and 706 cm^{-1} due to $\nu_{NH,}$ $\nu_{C=N/C=C,}$ $\nu_{C-N,}$ δ_{N-H} and δ_{C-H} respectively corresponding to organic moiety in the complex (Figure

2). It also displayed peaks at 1536 and 901 cm^{-1} due to $\nu_{N=O}$ and ν_{N-O}, thus confirming the coordination of nitrate to Fe(III). The $\nu_{NH,}$ and $\nu_{C=N/C=C}$ peaks due to ligand moiety in the encapsulated complex were masked by zeolite vibrational peaks. The peaks due to ν_{C-N} and δ_{N-H} at 1385, 1493 cm^{-1} respectively appeared as weak peaks and were shifted to higher wave number when compared to the $Fe(opbmzl)_2NO_3$ complex. The characteristic vibrational bands of zeolite framework in metal exchanged zeolite or zeolite encapsulated complex were not shifted inferring that the zeolite framework has remained unaffected upon metal exchange and encapsulation of the complex.

3.3 UV-vis DRS spectral studies

UV-visible diffuse reflectance spectral data of ligand, $Fe(opbmzl)_2NO_3$ and encapsulated complexes are compiled in table 2. The $Fe(opbmzl)_2NO_3$ complex exhibited intra-ligand transitions at 219, 233 and 290 nm due to $\varphi \rightarrow \varphi^*$, $\pi \rightarrow \pi^*$ and $n \rightarrow \pi^*$ transitions respectively. The LMCT band was observed at 331 nm and the weak d-d transition band at 474 nm due to $^6A_{1g} \rightarrow {}^4T_{1g}$ (G) transition of an octahedral Fe(III) complex. [55-56] The encapsulated complex displayed intra- ligand bands at 248 and 295 nm due to $\pi \rightarrow \pi^*$ and $n \rightarrow \pi^*$ transitions respectively. The LMCT band was observed at 366 nm, while the d-d transition band was observed at 505 nm, further confirming an octahedral coordination of Fe(III) within the supercage. The LMCT and d-d transitions in encapsulated complex were found to be red shifted as compared to the $Fe(opbmzl)_2NO_3$ complex. The shifting implied that the electronic transitions are remarkably influenced due to the interaction of the metal complexes within the walls of the zeolite framework. The shifting of bands is reasoned to the following facts; (i) ground and/or excited state of LMCT transition is altered by encapsulation of $Fe(opbmzl)_2(H_2O)_2$ complex; (ii) Fe^{3+}

ions may vary the negative charge density of the framework oxygen leading to the shift of the lower and higher energy bands.[51]

3.4 ESR spectral studies

The ESR spectra of $Fe(opbmzl)_2Y$ and FeY are unresolved (Figure 3). The ESR spectrum of Fe-Y was found to be isotropic with g values at 2.6 and 2.0 due to $Fe(H_2O)_6^{3+}$ in zeolite cage. However ESR spectrum of $Fe(opbmzl)_2Y$ showed a rhombic spectrum with g values at 4.7 and 2.6 indicating a distorted octahedral coordination of Fe(III) inside the zeolite cavity, characteristic of high spin d^5 Fe(III) in weak field environment. [57]

3.5 Thermal Analysis

TG profiles of Fe-Y, $Fe(opbmzl)_2NO_3$ and $Fe(opbmzl)_2Y$ are presented in Figure 4. The $Fe(opbmzl)_2NO_3$ complex underwent two-step decomposition. The first step (240-350 ºC) showed a weight loss of 10.8 % corresponding to the loss of nitrate ion and the second (350-970 ºC) to decomposition of the ligand moiety (42.7 %). The encapsulated complex also showed two-step decomposition profile. The first decomposition step (100-210 ºC) with a weight loss of 16.3 % corresponds to loss of water molecules (both adsorbed by zeolite and coordinated to Fe in the complex), while the second step (200-900 ºC) could be attributed to the loss of complex.

3.6 Electrochemical studies

Encapsulation of transition metal complex within the cavity of zeolite-Y transforms the host from insulator to redox active. Earlier reports have demonstrated two kinds of mechanism for electron transfer; intra-zeolite and extra-zeolite pathways. [58-59] For the complexes within the zeolite cavity, intra-zeolite mechanism is predominant. In order to account for the mechanism in the materials under present study, electrochemical behaviour of Fe-Y, $Fe(opbmzl)_2NO_3$ and $Fe(opbmzl)_2Y$ was investigated using 0.1 M TBAP as supporting electrolyte in DMF (Figure 5).

The cyclic voltammogram of Fe-Y showed two cathodic reduction peaks at -0.384 and -0.980 V corresponding to Fe(IV)/Fe(III) and Fe(III)/Fe(II) couples respectively. The relative anodic peaks were observed at -0.776 V for Fe(II)/Fe(III) and -0.208 V for Fe(III)/Fe(IV) couples (Figure 5a). The cyclic voltammograms of $Fe(opbmzl)_2NO_3$ were recorded both in solid as well as in solution mode. In solid mode, two cathodic peaks at -0.711 and -0.058 V for Fe(IV)/Fe(III) and Fe(III)/Fe(II) couples were noticed. The corresponding anodic peaks were seen at -0.299 V [Fe(II)/Fe(III)] and 0.125 V [Fe(III)/Fe(IV)]. The cyclic voltammogram in solution mode exhibited cathodic peaks at -0.551 and -0.522 V for Fe(IV)/Fe(III) and Fe(III)/Fe(II) couples. The relevant anodic peaks were observed at -0.170 and 0.447 V for Fe(II)/Fe(III) and Fe(III)/Fe(IV) respectively. In both the modes, redox peaks due to ligand were also observed.

The cyclic voltammogram of $Fe(opbmzl)_2$-Y exhibited low intense peaks that may be due of low concentration of the complex in the cavity. It also presented ligand redox peaks as observed in case of $Fe(opbmzl)_2NO_3$ complex (Figure 5b). The cathodic peaks were observed at -0.422 and 0.324 V for Fe(IV)/Fe(III) and Fe(III)/Fe(II) couples and the relevant anodic peaks were observed at -0.239 and 0.430 V for Fe(II)/Fe(III) and Fe(III)/Fe(IV) respectively.

Compared to non-encapsulated complex, the peaks were relatively broadened upon encapsulation which could be due to the interaction of metal complex with the walls of the zeolite cage. During the course of interaction, metal complex may perturb the active sites present within the zeolite, inducing different interaction energies and modify the redox potential at different places in the zeolite. [60] If there is any drastic decrease in peak currents for zeolite modified electrode, then the electron transfer occurs via an extra-zeolite mechanism. CV of the encapsulated complex showed no decrease in peak currents and found to be independent of scan rate accompanied with exceptional stability for prolonged time without any change in redox

potential values (Figure 5), which underscores the intra-zeolite electron transfer pathway (Figure 6). According to the previous reports, if the electron transfer occurs between the species within the cavities of zeolite, peak intensity increases without any prominent shift in peaks positions, termed as intra-zeolite mechanism. [61-63]

3.7 Catalytic Reactions

Influence of various reaction parameters on the probe reactions

In order to optimize the reaction conditions for maximum conversion, impact of distinct reaction parameters viz. substrate and catalyst concentration, substrate to oxidant ratio, reaction temperature, solvents polarity, nature and concentration of brominating agent (in case of oxidative bromination) were investigated in detail.

3.7.1 Oxidative bromination

3.7.1.1 Effect of reaction temperature

The effect of temperature on oxidative bromination was investigated by reiterating the reaction in the temperature range of 30-60 ℃ using 10 mmoles of aniline, 0.09 g of catalyst, 25 mmoles of H_2O_2 in 10 mL CH_3CN in presence of 11 mmoles of KBr as the brominating agent (Table S1). Though variation in temperature had little effect on the conversion of aniline (30 °C; 84.4 % and 60 °C; 88.0 %), decrease in regio-selectivity with increase in temperature was observed. This suggested that the aniline conversion was very susceptible to the reaction temperature and the most favorable temperature at which the aniline molecules had threshold energy to overcome the barrier in order to form p-bromoaniline was found to be 60 ℃.

3.7.1.2 Influence of solvents

The solvent not only influences the reaction rate by dissolving the reactant molecules and intermediates in the solution, but also stabilize or destabilize the transition state and alters the

concentration and distribution of intermediates formed during the reaction course at the active site of catalyst. It is also well known that using H_2O_2, oxidative bromination in acidic medium can be readily carried out. [64-65] The encapsulated complex Fe(opbmzl)$_2$-Y catalyzed oxidative bromination in common organic solvents in absence of acid. Thus in order to emphasize the role of catalyst on the reaction, various solvents in absence of an acid were used among which the reaction showed better conversion (84.4 %) in acetonitrile and the conversion followed the order; acetonitrile (84.4 %) > dichloroethane (76.0 %) > dichloromethane (74.3 %) > chloroform (70.5 %) (Table S1).

3.7.1.3 Influence of aniline concentration

Influence of aniline concentration (5, 7, 10, 15, 20 and 25 mmole) on oxidative bromination was examined to obtain maximum conversion and better regio-selectivity (Figure S1). It was observed that 10 mmoles of aniline gave maximum conversion (84.4 %) while further increase in concentration to 25 mmoles decreased the conversion (69.6 %). Increase in aniline concentration results in increase in competition between the aniline molecules for the active sites, thus decreasing conversion.

3.7.1.4 Influence of aniline: H_2O_2 mole ratio

Oxidative bromination of aniline was carried out by varying the content of H_2O_2 (from 1:1 to 1:3) by maintaining the other set of parameters constant (Figure S2). The bromination was maximum for 1:2.5 molar ratio. With further increase in molar ratio to 1:3, both % aniline conversion (76.9 %) and selectivity towards 4-bromoaniline decreased (76.8 %). It is well known that with increase in H_2O_2 content, the reaction medium gets diluted due to presence of water.

3.7.1.4 Influence of nature and concentration of brominating agent

The effect of brominating agent was also studied for the oxidative bromination of aniline using H_2O_2 as oxidant and MBr (M = Li, Na, K) as a bromine source (Figure S3). Among them, KBr has been found to be the most efficient bromine source (84.4 % conversion) with better regio-selectivity towards p-product (95.6 %). Though sodium bromide gave good conversion (79.4 %), regio-selectivity decreased (74.3 %) while LiBr gave very poor conversion (38.7 %).

In order to account for the effect of concentration of KBr, three different concentrations were employed (5.5, 11.0 and 22.0 mmoles). The % aniline conversion and product selectivity was maximum for 11.0 mmoles of KBr (84.4 %) (Table S5).

3.7.1.5 Influence of catalyst concentration

The influence of catalyst concentration on oxidative bromination was investigated for four different concentrations of catalyst viz., 0.070, 0.080, 0.090 and 0.100 g (Figure S4). Conversion was highest for 0.090 g of catalyst (84.4 %) and decreased slightly above this concentration (84.1 % for 0.100 g). With increase in the concentration of catalyst, the number of active sites also increases. This may decrease the conversion, as the oxidant and substrate may bind to different sites. For effective conversion, both substrate and oxidant have to bind to the same active site.

3.7.1.6 Comparison of catalytic acitivity with NaY, FeY and $Fe(opbmzl)_2NO_3$

The catalytic activity of encapsulated complex was compared with that of Fe-Y and $Fe(opbmzl)_2NO_3$ (Figure 7). The % aniline conversion and selectivity towards para-product followed the order; $Fe(opbmzl)_2$-Y (84.4, 95.6 %) > $Fe(opbmzl)_2NO_3$ (76.5, 87.9 %) > Fe-Y (72.1, 74.6 %) (Figure 7). A blank reaction was also carried out in absence of the catalyst, wherein 7.4 % conversion was observed at optimized conditions.

The reaction was carried out using NaY, wherein 12.9 % aniline conversion with 34.6 % selectivity towards para-product was observed. This lower conversion explains the influence of redox active transition metal complex in the zeolite.

3.7.1.6 Influence of nature of substrates

Oxidative bromination of few aromatics was also carried out at the optimized conditions of aniline (Table 3). As ^{-}OH, OCH_3, NH_2 and CH_3 groups are considered as ortho and para directing and activating groups, the activated aromatic substrates like phenol, anisole, aniline and toluene showed excellent para-selectivity and high conversion yielding respective mono-selective products.

Benzene being less active towards electrophilic substitution reaction, showed lower conversion (29.3 %), while deactivated aromatic ring such as nitrobenzene also gave lower conversion under optimized conditions (18.5 %). 4-substituted aromatics such as 4-aminophenol was selectively converted to 2-bromo derivative. The NMR spectra of brominated products is presented in Figure S5 (a-g).

3.7.2 Cyclohexane oxidation

Another model reaction like cyclohexane oxidation was also performed in the similar way and various reaction parameters were optimized in the sequence as discussed earlier.

3.7.2.1 Influence of temperature

Effect of temperature was also investigated for cyclohexane oxidation maintaining the other parameters constant (Table S2). It was observed that, with increase in temperature from 30 to 70° C, cyclohexane conversion also advanced subsequently from 22.9 to 55.6 % along with increase in selectivity towards cyclohexanone (41.7 to 57.4 %). Thus, 70 °C was considered as optimum for better cyclohexane conversion.

3.7.2.2 Influence of solvents

The nature of solvent also influences the catalytic activity. It was observed that among the solvents used, acetonitrile showed better conversion (55.6 %) and good selectivity towards cyclohexanone (57.4 %) owing to its good coordination ability (Table S2). It was observed that the cyclohexane oxidation was better in chloroform (51.2%) and least in methanol (38.6 %) which could be due to non-polar nature of chloroform.

3.7.2.3 Influence of cyclohexane concentration

The initial concentration of cyclohexane was found to be the key factor in the oxidation process. The conversion rate increased proportionately with enhancement in the cyclohexane concentration at the initial stages (30 - 60 mmoles) and declined at later stages. As shown in Table S2, cyclohexane conversion followed the progression; 30 mmole (42.3 %) > 40 mmole (46.9 %) > 70 mmole (49.1 %) > 50 mmole (49.9 %) > 60 mmole (55.6 %).

Hence, 60 mmoles was considered to be optimum concentration of cyclohexane for maximum conversion.

3.7.2.4 Influence of cyclohexane: H_2O_2 mole ratio

The effect of cyclohexane: H_2O_2 molar ratio was investigated for four different molar ratios; 1:1, 1:2, 1:2.5 and 1:3 (Table S2). The conversion of cyclohexane showed an increasing trend with increase in molar ratio from 1:1 (29.5 %) to 1:2.5 (55.6 %). However above 1:2.5 molar ratio, the percentage conversion and cyclohexanone selectivity almost remained constant.

The above result suggests that a large amount of oxidant is not an essential criterion in improving the catalytic performance of the catalyst. Thus 1:2.5 molar ratio was optimal for the reaction.

3.7.2.5 Influence of catalyst concentration

The effect of catalyst concentration was also evaluated for 3 different concentrations (0.120, 0.130 and 0.140 g) maintaining other parameters constant (Table S2). It was observed that the maximum conversion (55.6 %) was obtained when 0.130 g of catalyst was used. When 0.120 g of catalyst was used, the conversion was only 41.9 %. The conversion decreased when the catalyst concentration was increased to 0.140 g (50.3 %)

3.7.2.5 Comparison of catalytic activity of $Fe(opbmzl)_2$-Y with Na-Y, FeY and $Fe(opbmzl)_2NO_3$ towards cyclohexane oxidation

To further establish the significance of the encapsulated complex, its performance was compared with FeY, Na-Y and $Fe(opbmzl)_2NO_3$. Cyclohexane conversion followed the order; $Fe(opbmzl)_2Y$ (55.6 %) > $Fe(opbmzl)_2NO_3$ (51.3 %) >Fe-Y (47.9 %), while cyclohexanone selectivity followed the order; $Fe(opbmzl)_2Y$ (57.4 %) > Fe-Y (54.4 %) > $Fe(opbmzl)_2NO_3$ (50.7 %) (Figure 8).

3.7.3 Ethylbenzene oxidation

The encapsulated complex was used to catalyze the oxidation of ethylbenzene, by H_2O_2, to give acetophenone and benzaldehyde as major products and benzoic acid as minor product.

3.7.3.1 Influence of temperature

The effect of temperature on the oxidation of ethylbenzene was studied at five different temperatures (viz. 30, 40, 50, 60 and 70 ºC) with 4.2 g of ethylbenzene (40 mmol), 9.1 g of aqueous 30% H_2O_2 (80 mmol), and 0.001 g of catalyst in 10 mL of acetonitrile (Table S3). The performance of catalyst (conversion 62.7 %) increased with temperature up to 60 °C, but at 70 ºC though conversion increased marginally (65.9 %), the selectivity towards acetophenone and benzaldehyde drastically decreased with increase in selectivity towards benzoic acid (56.3 %).

Thus, 60 ºC was the required temperature to get maximum selectivity towards acetophenone (53.6 %).

3.7.3.2 Influence of solvents

The catalytic activity was examined using acetonitrile, dichloromethane, methanol, acetone and ethanol. The ethylbenzene conversion was maximum in acetonitrile. The order of conversion was as follows; acetonitrile (62.7 %) > acetone (51.3 %) > ethanol (47.3 %) > methanol (43.5 %) > dichloromethane (36.2 %) (Table S3).

3.7.3.3 Influence of ethylbenzene concentration

The effect of ethylbenzene concentration on conversion was studied maintaining the other optimized conditions constant (Table S3). It was observed that conversion increased with increase in concentration of ethylbenzene from 30 mmoles (45.9 %) to 40 mmoles (62.7 %). Further increase in concentration to 50 mmoles, both conversion and selectivity towards acetophenone decreased (52.3 % and 31.5 % respectively).

3.7.3.4 Influence of ethylbenzene: H_2O_2 mole ratio

The influence of H_2O_2 concentration on the oxidation of ethylbenzene as a function of time has been studied considering ethylbenzene: H_2O_2 molar ratios of 1:1, 1:2 and 1:3 (Table S3). For a fixed amount of ethylbenzene (4.2 g, 40 mmol), catalyst (0.110 g) and acetonitrile (10 mL), the conversion of ethylbenzene was 62.7 % in 6h of reaction time at 60 ºC for the ethylbenzene to H_2O_2 molar ratio of 1:2. Increasing this ratio to 1:3 increased the conversion to 69.9 % but the selectivity towards acetophenone decreased drastically (23.3 %).

3.7.3.5 Influence of catalyst concentration

Among different concentrations of catalyst used, conversion was low (51.6 %) for 0.100 g of catalyst with 4.2 g of ethylbenzene (40 mmol) and 9.1 g of H_2O_2 (80 mmol) in 10 mL of

acetonitrile for 6 h (Table S3). Increasing the catalyst amount to 0.110 g, improved this conversion to 62.7 %. Further increment of catalyst amount to 0.120 g slightly reduced the conversion (59.3 %), while selectivity towards acetophenone decreased drastically to 19.3 %.

3.7.3.6 Comparison with NaY, FeY and $Fe(opbmzl)_2NO_3$

The catalytic activity of the encapsulated complex was compared with that of $Fe(opbmzl)_2NO_3$ complex and Fe-Y (Figure 9). $Fe(opbmzl)_2NO_3$ complex showed 58.6 % conversion of ethylbenzene under the above optimized conditions with selectivity towards acetophenone and benzaldehyde was 42.1 and 47.3 % respectively. Fe-Y showed 51.2 % conversion with 39.6 % acetophenone selectivity. The zeolite framework in encapsulated complex has influenced on the selectivity of oxidation products of ethylbenzene in that using H_2O_2 as oxidant, acetophenone was always obtained as the major product (53.6 % selectivity).

3.7.4 Test for recyclability and heterogeneity of the reaction

The recyclability of the catalyst has been tested for the probe reactions. The catalyst separated from the reaction mixture after the catalytic reaction and washed with acetonitrile, dried and subjected to further catalytic reactions under respective optimized conditions. No appreciable loss in the activity in all cases suggested that the catalyst is active even after second cycle with small decrease in the activity after third run (Table 4). To check the heterogeneous nature of the catalyst, reactions were carried out for 2 h at optimized conditions, catalyst was filtered and the reaction was continued for another 2h. The gas chromatographic analyses showed no further increment in the conversion confirming that the reactions did not proceed upon removal of the solid catalyst and the reactions were truly heterogeneous.

Comparison of the catalytic activity of $Fe(opbmzl)_2$-Y with other reported systems revealed that the present catalyst exhibits good conversion of aniline (84.4 %), cyclohexane

(55.6) and ethylbenzene (62.7%) with good selectivity towards para-substituted product (in this case 4-bromoaniline) (95.6%), cyclohexanone (42.6%) and acetophenone (53.6%) when compared to reported systems (Table 5-7) [66-80].

3.7.5 Mechanistic studies

Oxidative bromination and oxidation of ethylbenzene was found to occur via ionic mechanism which was confirmed by carrying out the reactions in the presence of radical abstractor BHT (Schemes 2-4). In case of cyclohexane oxidation, the reaction did not proceed in presence of BHT, which could be considered as an evidence for radical mechanism (Scheme 3).

To establish the possible reaction pathway for non-encapsulated $Fe(opbmzl)_2NO_3$ complex, the complex was treated with H_2O_2 and progress of the reaction was monitored by UV-visible absorption spectroscopy (Figure 10). The titration of DMF solution of $[Fe(opbmzl)_2NO_3]$ with one-drop portions of 30% H_2O_2 dissolved in DMF (10^{-3} M) resulted in the slight shift of 291 nm band to 293 nm along with the increase in its intensity, while band at 335 nm decreased in intensity with appearance of other band at 359 nm. UV band at 416 was broadened and shifted to 436 nm. These changes may be due to the formation of intermediate $NO_3(opbmzl)_2Fe\text{-}OOH$ which finally transfers oxygen to the substrates. [81-83]

Similarly, reaction between H_2O_2 and complex in the zeolite cavity is expected to lead to the formation of $[(H_2O)(opbmz)_2Fe\text{-}OOH]$ intermediate which may further react with the coordinated substrate to give oxidized products by homolytic cleavage of O-O bond of H_2O_2 resulting in OH radicals or by heterolytic cleavage leading to oxidation of ethylbenzene and oxidative bromination, while in case of cyclohexane oxidation the reaction proceeded with homolytic cleavage of the intermediate.

For further confirmation for the type of mechanism in the probe reactions and to check for homolytic versus heterolytic scission of the peroxide O-O bond, the oxidative bromination and oxidation of cyclohexane and ethylbenzene under the optimized reaction conditions were carried out using methyl-1-phenyl-2-propyl hydroperoxide (MPPH) as a mechanistic probe. It is known that, if the reaction proceed via heterolytic cleavage of the O-O bond, the reaction with MPPH and the catalyst should give 2-methyl-1-phenyl-2-propanol. On the other hand, homolytic cleavage of the hydroperoxide leads to a radical mechanism yielding acetone, benzyl alcohol, and benzaldehyde as some of the β-scission fragmentation products. [84- 85] The reactions were carried out using MPPH (1.7 g) under respective optimized conditions and the reaction products were analyzed by GC which revealed the presence of 2-methyl-1-phenyl-2-propanol in case of oxidative bromination and oxidation of ethylbenzene, whereas in case of cyclohexane oxidation, the product GC analysis revealed the presence of cyclohexanol, cyclohexanone, benzyl alcohol, benzaldehyde and unreacted cyclohexane indicating that oxidative bromination and oxidation of phenol, styrene and ethylbenzene occurred by heterolytic cleavage of the O-O bond while oxidation of cyclohexane took place by homolysis of O-O bond of hydroperoxide.

The $[(H_2O)(opbmz)_2Fe\text{-}OOH]$ formed in case of oxidative bromination would later react with Br^- ion to liberate HOBr that may bind to the Fe center and attack the substrate by an electrophilic attack (Br^+) to give bromo-product. [64, 86-88]

4.0 Conclusion

Encapsulation of bis[2,2'-hydroxyphenylbenzimidazole]Fe(III) complex within the cavity of zeolite-Y was supported by reduction in pore volume. Presence of ligand and complex peaks in the IR spectrum with red-shift of LMCT transitions in UV-vis DRS spectrum further supported

this fact. From UV-vis and ESR spectral data, an octahedral coordination around Fe(III) in the encapsulated complex was assigned. An increased current without any change in peak potential with respect to difference in scan rates in the cyclic voltammogram of the complex described an intra-zeolite electron transfer within the cavity. The encapsulated complex showed higher catalytic activity and selectivity in all the reactions as compared to $Fe(opbmzl)_2NO_3$. Leaching tests indicated that the catalytic reactions were truly heterogeneous in nature. The catalyst can be reused three times without significant decrease in its activity.

Associated Content

Supporting Information

Analytical data related to effect of KBr concentration, brominating agents (oxidative bromination), solvent, temperature, substrate:H_2O_2 mole ratio, substrate concentration and time on the reactions rate.

Acknowledgement

Authors thank Department of Chemistry, Bangalore University for providing instrumentation facilities and Prof. P. V. Kamath and his research student G. K. Kiran for cyclic voltammetric studies.

Funding

The authors declare no competing financial interest.

References

1 Balkus K. J. Jr, Alexei G. G, Zeolite encapsulated metal complexes. *Inclusion Phenom. Mol. Recognit. Chem.* **21**: 159-184 (1995).

2 Gupta K. C, Sutar. A. K, Catalytic activities of Schiff base transition metal complexes, *Coord. Chem. Rev.* **252**: 1420-1450 (2008).

3 Salavati-Niasari. M, Nanoscale microreactor-encapsulation 14-membered nickel(II) hexamethyl tetraaza: synthesis, characterization and catalytic activity. *J. Mol. Catal. A: Chem.* **229**: 159-164 (2005).

4 Weckhuysen. B. M, Verberckmoes. A. A, Vannijvel. I. P, Pelgrims. J. A, Buskens. P. L, Jacobs. P. A, Schoonheydt. R. A. In zeolites included copper-histidine complexes as mimetics of natural copper enzymes. *Angew. Chem. Int. Ed. Engl.* **34**: 2652-2654 (1995).

5 Grommen. R, Manikandan. P, Gao. Y, Shane. T, Shane. J. J, Schoonheydt. R. A, Weckhuysen. B. M, Goldfarb. D. Geometry and Framework Interactions of Zeolite-Encapsulated Copper(II)-Histidine Complexes. *J. Am. Chem. Soc.* **122**: 11488-11496 (2000).

6 Ledney. M, Dutta. P. K. Oxidation of Water to Dioxygen by Intrazeolitic $Ru(bpy)_3^{3+}$. *J. Am. Chem. Soc*. **117**: 7687-7695 (1995).

7 Schulz-Ekloff. G, Ernst. S, Ertl. G, Knözinger. H (Eds.), Handbook of Heterogeneous Catalysis, VCH, Weinheim, Germany. 374-375 (1997).

8 Wischang. D, Brucher. O, Hartung. Bromoperoxidases and Functional Enzyme Mimics for Oxidative Bromination - A Sustainable Synthetic Approach. J. *Coord. Chem. Rev.* **255**: 2204-2217 (2011).

9 Clark. J. Green chemistry: challenges and opportunities. *Green Chem*. **1**: 1-8 (1999).

10 Pingali. S. R. K, Madhav M, Jursic. B. S. An efficient regioselective NBS aromatic bromination in the presence of an ionic liquid. *Tetrahedron Lett.* **51**: 1383-1385 (2010).

11 Stropnik. T, Bombek. S, Kocevar. M, Polanc. S. Regioselective bromination of activated aromatic substrates with a $ZrBr_4$/diazene mixture. *Tetrahedron Lett.* **49:** 1729-1733 (2008).

12 Zolfigol. M. A, Chehardoli. G, Salehzadeh. S, Adams. H, Ward. M. D. {[K.18-Crown-6]Br_3}*n*: a unique tribromide-type and columnar nanotube-like structure for the oxidative coupling of thiols and bromination of some aromatic compounds. *Tetrahedron Lett.***48**: 7969−7973 (2007).

13 Borikar. S. P, Daniel. T, Paul. V. An efficient, rapid, and regioselective bromination of anilines and phenols with 1-butyl-3-methylpyridinium tribromide as a new reagent/solvent under mild conditions. Tetrahedron Lett. **50**: 1007−1009 (2009).

14 Chiappe. C, Leandri. E, Pieraccini. D. Highly efficient bromination of aromatic compounds using 3-methylimidazolium tribromide as reagent/solvent. *Chem. Commun*. 2536−2537 (2004).

15 Zhang-Gao. L, Zhen-Chu. C, Yi. H, Qin-Guo. Z. [bmim]Br_3 as a New Reagent for Regioselective Monobromination of Arylamines under Solvent-Free Conditions. *Synthesis*. **17**: 2809−2812 (2004).

16 Salazar. J, Dorta. R. Pentylpyridinium Tribromide: A Vapor Pressure Free Room Temperature Ionic Liquid Analogue of Bromine. *Synlett*. **7**: 1318-1320 **(**2004).

17 Hosseinzadeh. R, Tajbakhsh. M, Mohadjerani. M, Lasemi. Z. Efficient and Regioselective Bromination of Aromatic Compounds with Ethylenebis(*N*-methylimidazolium) Ditribromide (EBMIDTB). *Synth. Commun.* **40**: 868-876 (2010).

18 Al-Zoubi. R. M, Hall. D. G. Mild Silver(I)-Mediated Regioselective Iodination and Bromination of Arylboronic Acids. *Org. Lett*. **12**: 2480−2483 (2010).

19 Jacquesy. J, Jouannetaud. M, Makani. S. *meta*-Bromination of phenols in superacids. *J. Chem. Soc. Chem. Commun*. **3**: 110−111 (1980).

20 Gnaim. J. M, Sheldon. R. A. Synthesis of fused α-methylene-γ-butyrolactone derivatives through pyridine-induced addition of phenols to dimethyl acetylenedicarboxylate. *Tetrahedron Lett*. **46**: 4465− 4468 (2005).

21 Smith. K, El-Hiti. G. A, Hammond. M. E. W, Bahzad. D, Li. Z, Siquet. C. Highly efficient and selective electrophilic and free radical catalytic bromination reactions of simple aromatic compounds in the presence of reusable zeolites. *J. Chem. Soc. Perkin Trans.* **116**: 2745−2752 (2000).

22 Naik. S. N, Naik. D. R. R, Rao. M. M. High purity 4.4′- isopropylidene-bis-(2.6 dibromophenol) and process for the preparation of such high purity 4.4′-isopropylidene-bis-(2.6 dibromophenol). U.S. Patent 6.613.947 (2003).

23 Choudary. B. M, Someshwar. T, Reddy. C. V, Kantam. M. L, Jeevaratnam. K, Sivaji. L. V. The first example of bromination of aromatic compounds with unprecedented atom economy using molecular bromine. *Appl. Catal. A.* **251**: 397−409 (2003)

24 Park. M. Y, Yang. S. G, Jadhav. V, Kim. Y. H. Practical and regioselective brominations of aromatic compounds using tetrabutylammonium peroxydisulfate. *Tetrahedron Lett*. **45**: 4887−4890 (2004).

25 Conte. V, Floris. B. Vanadium catalyzed oxidation with hydrogen peroxide. *Inorg. Chim. Acta.* **363**: 1935-1946 (2010).

26 Moriuchi. T, Yamaguchi. M, Kikushima. K, Hirao. T. An efficient vanadium-catalyzed bromination reaction. *Tetrahedron Lett*. **48**: 2667-2670 (2007).

27 Conte. V, Floris. B, Galloni. P, Silvagni. A. Sustainable vanadium(V)-catalyzed oxybromination of styrene: Two-phase system versus ionic liquids. *Pure Appl. Chem*. **77**: 1575-1581 (2005).

28 Sels. B. F, De Vos. D. E,, Jacobs. P. A. Use of WO_4^{2-} on Layered Double Hydroxides for Mild Oxidative Bromination and Bromide-Assisted Epoxidation with H_2O_2. *J. Am. Chem. Soc.* **123**: 8350-8359 (2001).

29 Sels. B. F, De Vos. D. E, Buntinx. M, Jacobs. P. A. Transition metal anion exchanged layered double hydroxides as a bioinspired model of vanadium bromoperoxidase. *J. Catal.* **216**: 288-297 (2003).

30 Reynolds. M. S, BabinskiK. J, Bouteneff. M. C, Brown. J. L, Campbell. R. E, Cowan. M. A, Durwin. M. R, Foss. T, O'Brien. P, Penn. H. R. Kinetics of bromide oxidation by peroxo complexes of molybdenum(VI) and tungsten (VI). *Inorg. Chim. Acta.* **263**: 225-230 (1997).

31 Sinha. J, Layek. S, Mandal. G. C, Bhattacharjee. M. A green Hunsdiecker reaction: synthesis of beta-bromostyrenes from the reaction of alpha,beta-unsaturated aromatic carboxylic acids with KBr and H_2O_2 catalysed by $Na_2MoO_4.2H_2O$ in aqueous medium. *Chem. Commun.* 1916-1917 (2001).

32 Podgorsek. A, Zupan. M, Iskra. J. Oxidative halogenation with "green" oxidants: oxygen and hydrogen peroxide. *Angew. Chem. Int. Ed.* **48**: 8424-8450 (2009).

33 Maurya. M. R, Khan. A. A, Azam. A, Ranjan. S, Mondal. N, Kumar. A, Avecilla. F, Pessoa. J.C. Vanadium complexes having $[V^{IV}O]^{2+}$ and $[V^{V}O_2]^{+}$ cores with binucleating dibasic tetradentate ligands: Synthesis, characterization, catalytic and antiamoebic activities. *Dalton Trans.* **39**: 1345-1360 (2010).

34 Maurya. M. R, Sikarwar. S, Joseph. T, Manikandan. P, Halligudi. S.B. Synthesis, characterization and catalytic potentials of polymer anchored copper(II), oxovanadium(IV) and dioxomolybdenum(VI) complexes of 2-(α-hydroxymethyl)benzimidazole. *React. Funct. Polym*. **63**: 71-83 (2005).

35 Okuhara. T. Water-Tolerant Solid Acid Catalysts. *Chem. Rev*.**102**: 3641-3666 (2002).

36 Wilson. K, Clark. J. H. Solid acids and their use as environmentally friendly catalysts in organic synthesis. *Pure Appl. Chem.* **72**: 1313-1319 (2000).

37 Ji. J, Zhang. G, Chen. H, Wang. S, Zhang. G, Zhang. F, Fan. X. Sulfonated graphene as water-tolerant solid acid catalyst. *Chem. Sci.* **2**: 484-487 (2011).

38 Raja. R, Ratnasamy. P. Oxyhalogenation of aromatics over copper phthalocyanines encapsulated in zeolites. *J. catal.* **170**: 244–253 (1997).

39 Narender. N, Mohan. K.V.V.K, Reddy. R.V, Srinivasu. P, Kulkarni. S.J, Raghavan. K.V. Liquid phase bromination of phenols using potassium bromide and hydrogen peroxide over zeolites. *J. Mol. Catal. A: Chem.* **192**: 73–77 (2003).

40 Keith S. Highly regioselective, lewis acid-free electrophilic aromatic substitution. *J. Chem. Tech. Biotechnol.* **68:** 432-436 (1997).

41 Maurya. M. R, Saklani. H, Kumar. A, Chand S. Oxidative bromination of salicylaldehyde by potassium bromide/H_2O_2 catalysed by dioxovanadium(V) complexes encapsulated in zeolite–Y: a functional model of haloperoxidases. *Catal. Commun.* **5:** 563–568 (2004).

42 Titinchi. S. J. J, Willingh. G. V, Abbo. H. S, Prasad. R. Tri- and tetradentate copper complexes: a comparative study on homogeneous and heterogeneous catalysis over oxidation reactions. *Catal. Sci. Technol.* **5**: 325-338 (2015).

43 Kumar. R, Sithambarama. S, Suib. S. L. Cyclohexane oxidation catalyzed by manganese oxide octahedral molecular sieves-Effect of acidity of the catalyst. *J. Catal.* **262**: 304-313 (2009).

44 Trakarnpruk. W, Kanjina. W. Selective oxidation of ethylbenzene to acetophenone catalyzed by mixed oxide spinels derived from layered double hydroxides. *Mendeleev Commun.* **22**: 275-277 (2012).

45 Ian. C. C, Janet. C, John S. R, Duncan. J. M, James. H. C, Katherine. A. U. Environmentally friendly liquid phase oxidation:enhanced selectivity in the aerial oxidation ofalkyl aromatics, epoxidations and the Baeyer–Villiger oxidation using novel silica supported transition metal ions. J Chem Technol Biotechnol. **74:** 923-930 (1999)

46 Haitt R. R, Strachan W. M. J. The Effect of Structure on the Thermal Stability of Hydroperoxides. *J. Org. Chem.* ***28***: 1893–1894 (1963).

47 Hein. D.W, Alheim. R. J. The Use of Polyphosphoric Acid in the Synthesis of 2-Aryl- and 2-Alkyl-substituted Benzimidazoles, Benzoxazoles and Benzothiazoles. *J. Am. Chem. Soc*. **79**: 427-429 (1957).

48 Yuzo. N, Kasumi. Y, Akila. F. ESR spectra and reactivity towards catechol of iron(III) complexes with 2-(2-benzimidazolyl)phenol and its benzoxazole derivative. *Zeitschrift fuer naturfors chung B: Chem Sciences.* **45**: 1433-1436 (1990).

49 Bania. K. K, Deka. R. C. Experimental and Theoretical Evidence for Encapsulation and Tethering of 1,10-Phenanthroline Complexes of Fe, Cu, and Zn in Zeolite-Y. *J. Phys. Chem. C.* **116**: 14295-14310 (2012).

50 Salama. T. M, Ahmed. A. H, Bahy. Z. M. E. Y-type zeolite-encapsulated copper(II) salicylidene-p-aminobenzoic schiff base complex: Synthesis, characterization and carbon monoxide adsorption. *Micropor. Mesopor. Mater.* **89**: 251-259 (2006).

51 Bania. K. K, Bharali. D, Viswanathan. B, Deka. R. C. Enhanced Catalytic Activity of Zeolite Encapsulated Fe(III)-Schiff-Base Complexes for Oxidative Coupling of 2-Napthol. *Inorg. Chem.* **51:** 1657-1674 (2012).

52 Tanaka. K, Choo. C.K, Komatsu. Y, Hamaguchi. K, Yamaki. M, Itoh. T, Nishigaya. T. Nakata. R, Morimoto. K. Characterization and preparation of chained Si species in zeolite supercages. *J. Phys. Chem. B.* **108**: 2501-2508 (2004).

53 Bania. K. K, Deka. R. C. Zeolite-Y Encapsulated Metal Picolinato Complexes as Catalyst for Oxidation of Phenol with Hydrogen Peroxide, J. Phys. Chem. C. **117**: 11663-11678 (2013).

54 Mozgawa. W, Król. M, Barczyk. K, FT-IR studies of zeolites from different structural groups, *CHEMIK.* **65**: 667-674 (2011).

55 Lever. A. B. P, *Inorganic Electronic Spectroscopy, second ed., Elsevier, Amsterdam*, 1984.

56 Bhattacharjee. C. R, Goswami. P, Mondal. P. Synthesis, reactivity, thermal, electrochemical and magnetic studies on iron(III) complexes of tetradentate Schiff base ligands. *Inorg. Chim. Acta.* **387**: 86-92 (2012).

57 Viswanathan. R, Palaniandavar. M, Balasubramanian. T, Muthiah. P. T. Synthesis, structure, spectra and redox chemistry of iron(III) complexes of tridentate pyridyl and benzimidazolyl ligands. *J. Chem. Soc. Dalton Trans.* 2519-2525 (1996).

58 Bedioui. F, Roue. L, Briot. E, Devynck. J, Bell. S, Balkus. K. J. Jr. Electrochemistry of chemically modified zeolites: Discussion and new trends, *J. Electroanal. Chem*. **373**: 19-29 (1994).

59 Mesfar. k, Carre. B, Bedioui. F, Devynck. J. Electrochemistry of zeolite-encapsulated complexes. Part 4-Characterization of transition-metal polypyridinediyl and phenanthroline complexes entrapped in Y faujasite-type zeolite. *J. Mater Chem.* **3**: 873-876 (1993).

60 K. K. Bania and R. C. Deka, Influence of zeolite framework on the structure, properties, and reactivity of cobalt phenanthroline complex: A combined experimental and computational study, J. Phys. Chem. C.**115**: (2011) 9601-9607.

61 P. J. Carl, S. C. Larsen, EPR study of copper-exchanged zeolites: Effects of correlated g- and A-Strain, Si/Al Ratio, and parent zeolite, J. Phys. Chem. B. **104:** (2000) 6568-6575.

62 B. R. Shaw, K. E. Creasy, C. J. Lanczycki, J. A. Sargeant, M. Tirhado, Voltammetric response of zeolite-modified electrodes, J. Electrochem. Soc.**135:** (1988) 869-876.

63 R. Zhang, J. Ma, W. Wang, B. Wang, R. Li, Electrooxidation kinetics of hydrazine on Y-type zeolite encapsulated Ni(II)(salen) complex supported on graphite modified electrode, J. Electroanal. Chem. **643:** (2010) 31-38.

64 Maurya. M. R, Kumara. U, Manikandan. P. Polymer supported vanadium and molybdenum complexes as potential catalysts for the oxidation and oxidative bromination of organic substrates. *Dalton Trans.* 3561–3575 (2006).

65 Kikushima. K, Moriuchi. T, Hirao. T. Mechanistic insights into iron porphyrin-catalyzed olefin epoxidation by hydrogen peroxide: Factors controlling activity and selectivity. *Tetrahedron.* **66**: 6906-6911 (2010).

66 Islam. S. M, Anupam Singha Roy. K. G, Salam. N, Chatterjee. T. *J Inorg Organomet Polym* **24**:457–467 (2014).

67 Nishina. Y, Takami. K. Bromination of aromatic compounds using an Fe_2O_3/zeolite catalyst. *Green Chem*. **14**: 2380–2383 (2012).

68 Ronghe. Lin, Yunjie. D, Leifeng G, Wenda. D, Junhu. W, Tao. Z. Efficient and stable silica-supported iron phosphate catalysts for oxidative bromination of methane. *J. Catal.* **272:** 65–73 (2010)

69 Runqin. W, Ronghe. L, Yunjie D, Jia. L, Junhu. W, Tao. Z. Structure and phase analysis of one-pot hydrothermally synthesized FePO4-SBA-15 as an extremely stable catalyst for harsh oxy-bromination of methane. *Appl. Catal. A: Gen*. **453**: 235– 243 (2013).

70 Maria. C. E, Enrique. G. O, Heiddy. M, Cla´udio. D, S´ılvia. M. S, Egues, Christiane. F, Adailton. J. B, Valderes. D, Antunes. O. A. C. Catalytic oxidation of cyclohexane by a binuclear Fe(III) complex biomimetic to methane monooxygenase. *J. Inorg. Biochem.* **99**: 2054–2061 (2005).

71 Wagner. A. C, Martin. W, Ulf. S. Iron and copper immobilised on mesoporous MCM-41 molecular sieves as catalysts for the oxidation of cyclohexane. *J. Mol. Catal. A: Chem.* **144**: 91–99 (1999).

72 Natasha. G, Tebello. N. Iron perchlorophthalocyanine and tetrasulfophthalocyanine catalyzed oxidation of cyclohexane using hydrogen peroxide, chloroperoxybenzoic acid and *tert*-butylhydroperoxide as oxidants. *J. Mol. Catal. A: Chem.* **179**: 113–123 (2002).

73 Parida. K. M, Mitarani. S, Sudarshan. S. Iron perchlorophthalocyanine and tetrasulfophthalocyanine catalyzed oxidation of cyclohexane using hydrogen peroxide,

chloroperoxybenzoic acid and *tert*-butylhydroperoxide as oxidants. *J. Mol. Catal. A: Chem.* **329**: 7–12 (2010).

74 Can. C. G, Gang. H, Xiao. B. Z, Dong. C. G. Catalysis of chitosan-supported iron tetraphenylporphyrin for aerobic oxidation of cyclohexane in absence of reductants and solvents. *Appl. Catal. A: Gen*. **247**: 261–267 (2003).

75 Chetan. K. M, Parthiv. M. T. Zeolite-Y entrapped Ru(III) and Fe(III) complexes as heterogeneous catalysts for catalytic oxidation of cyclohexane reaction, *Arab. J. Chem* (2013), 10.1016/j.arabjc.2013.03.016

76 Mduduzi. N. C, Holger. B. F, Muhammad. D. B. A study of Fe(III)TPPCl encapsulated in zeolite NaY and Fe(III)NaY in the oxidation of n-octane, cyclohexane, 1-octene and 4-octene. *Reac Kinet Mech Cat* **111:**737-750 (2014)

77 Habibia. D, Farajia. A. R, Arshadib. M, Fierroc. J. L. G. Characterization and catalytic activity of a novel Fe nano-catalyst as efficient heterogeneous catalyst for selective oxidation of ethylbenzene, cyclohexene, and benzylalcohol. *J. Mol. Catal. A: Chem.* **372** :90-99 (2013)

78 Shi. L, Shang. R. Z, Qing. D. A, Ming. H. L, Yu. S, Xiao. W. S. Designed synthesis of multifunctional Fe_3O_4@SiO_2–NH_2@CS–Co(II) towards efficient oxidation of ethylbenzene. *Mater. Res. Bull.* **60:** 665–673 (2014).

79 Jin. L, Hao. Y, Hongjuan. W, Feng. P. Enhancing the catalytic activity of carbon nanotubes by filled iron nanowires for selective oxidation of ethylbenzene. *Catal. Comm.* **51**:77–81 (2014).

80 Wang. R, Wang. H, Wang. X, Lei. C and Shi. X. Immobilization of Transition-metal Hydroxamates on Polystyrene Resins: Effective Biomimetic Heterogeneous Catalysts for Aerobic Oxidation of Ethylbenzene. Chem. Res. Chin. Univ. **31:** 835-840 (2015).

81 Stephenson. N. A, Bell. A. T. Mechanistic insights into iron porphyrin-catalyzed olefin epoxidation by hydrogen peroxide: Factors controlling activity and selectivity. *J. Mol. Catal. A: Chem*. **275**: 54-62 (2007).

82 Lubben. M, Meetsma. A, Wilkinson. E. C, Feringa. B, Que Jr. L. Nonheme Iron Centers in Oxygen Activation: Characterization of an Iron(III) Hydroperoxide Intermediate. *Angew. Chem. Int. Ed. Engl.* **34**: 1512-1514 (1995).

83 Bernal. I, Jensen. I. M, Jensen. K. B, McKenzie. C. J, Toftlund. H, Tuchagues. J. Iron(II) complexes of polydentate aminopyridyl ligands and an exchangeable sixth ligand; reactions with peroxides. Crystal structure of $[FeL^1(H_2O)][PF_6]_2 \cdot H_2O$ [L^1=*N*,*N*′-bis-(6-methyl-2-pyridylmethyl)-*N*,*N*′-bis(2-pyridylmethyl)ethane-1,2-diamine]. *J. Chem. Soc. Dalton Trans.* 3667-3675 (1995).

84 Sorokin A. B, Mangematin. S, Pergrale. C. Selective oxidation of aromatic compounds with dioxygen and peroxides catalyzed by phthalocyanine supported catalysts. J. Mol. Catal. A: Chem. **182–183**: 267-281 (2002).

85 Yiu S. M, Man. W, Lau. T. Efficient Catalytic Oxidation of Alkanes by Lewis Acid/$[Os^{VI}(N)Cl_4]^-$ Using Peroxides as Terminal Oxidants. Evidence for a Metal-Based Active Intermediate. J. Am. Chem. Soc. **130**: 10821-10827 (2008).

86 Rothenberg. G, Clark. J. H. Vanadium-Catalysed Oxidative Bromination Using Dilute Mineral Acids and Hydrogen Peroxide: An Option for Recycling Waste Acid Streams. *Organic Process Research & Developmen.* **4**: 270-274 (2000).

87 Sivey. J. D, M. A. Bickley, Daniel A. V. Contributions of BrCl, Br_2, BrOCl, Br_2O, and HOBr to Regiospecific Bromination Rates of Anisole and Bromoanisoles in Aqueous Solution. *Environ. Sci. Technol*. **49**: 4937−4945 (2015).

88 Hideyasu C, Yutaka O, Hiroyasu O. Production mechanism of active species on the oxidative bromination following perhydrolase activity. *J. Phys. Org. Chem*. **29**: 84–91 (2016).

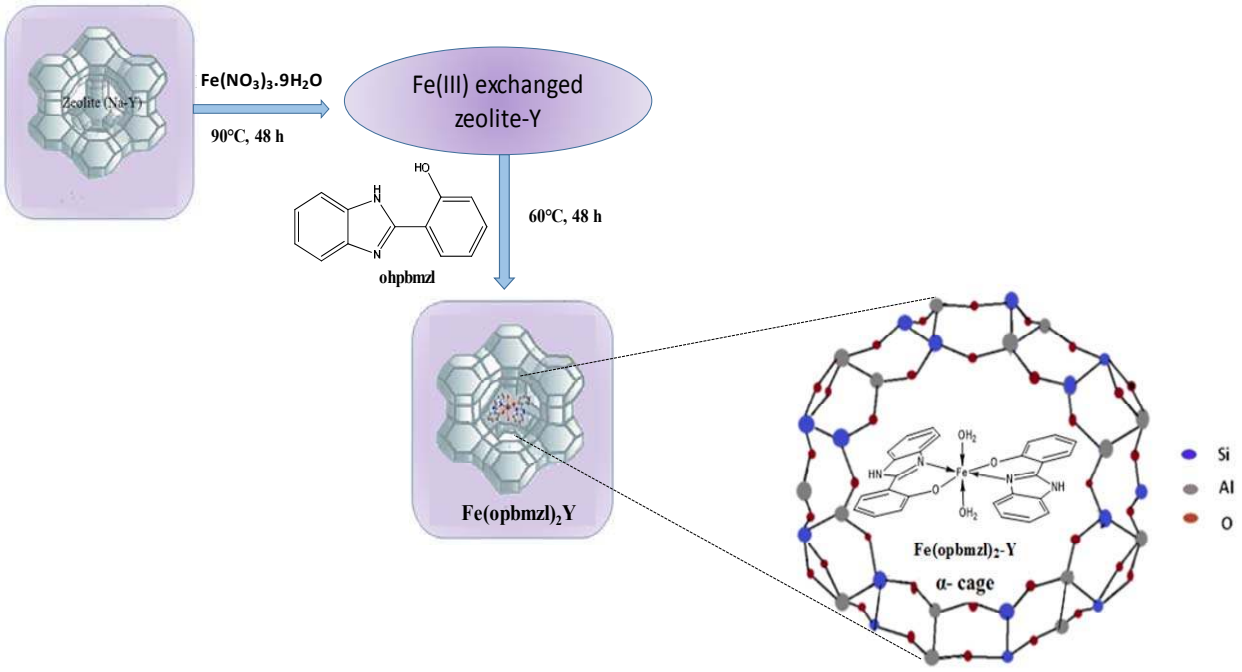

Scheme 1: Preparative route for $Fe(opbmzl)_2$-Y

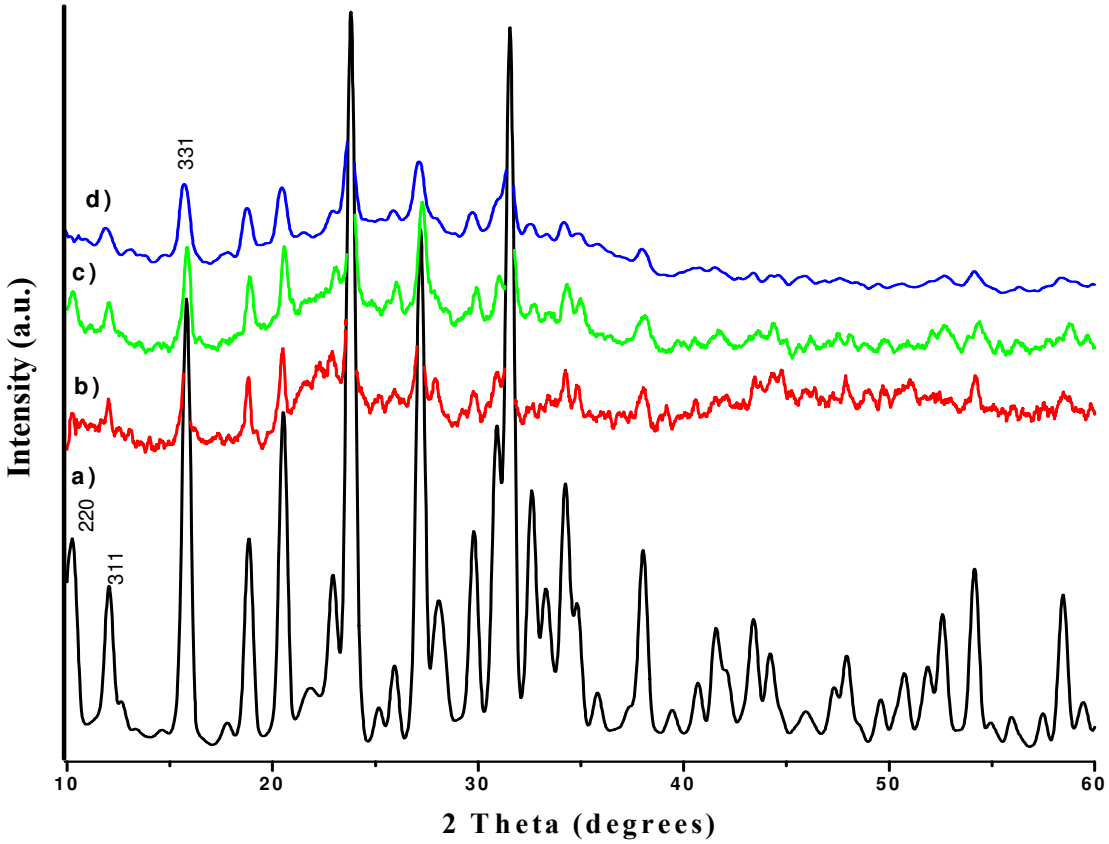

Figure 1: XRD pattern of (a) Na-Y, (b) Fe(opbmzl)$_2$-Y, (c) Fe-Y and (d) Fe(opbmzl)$_2$-Y (Reused)

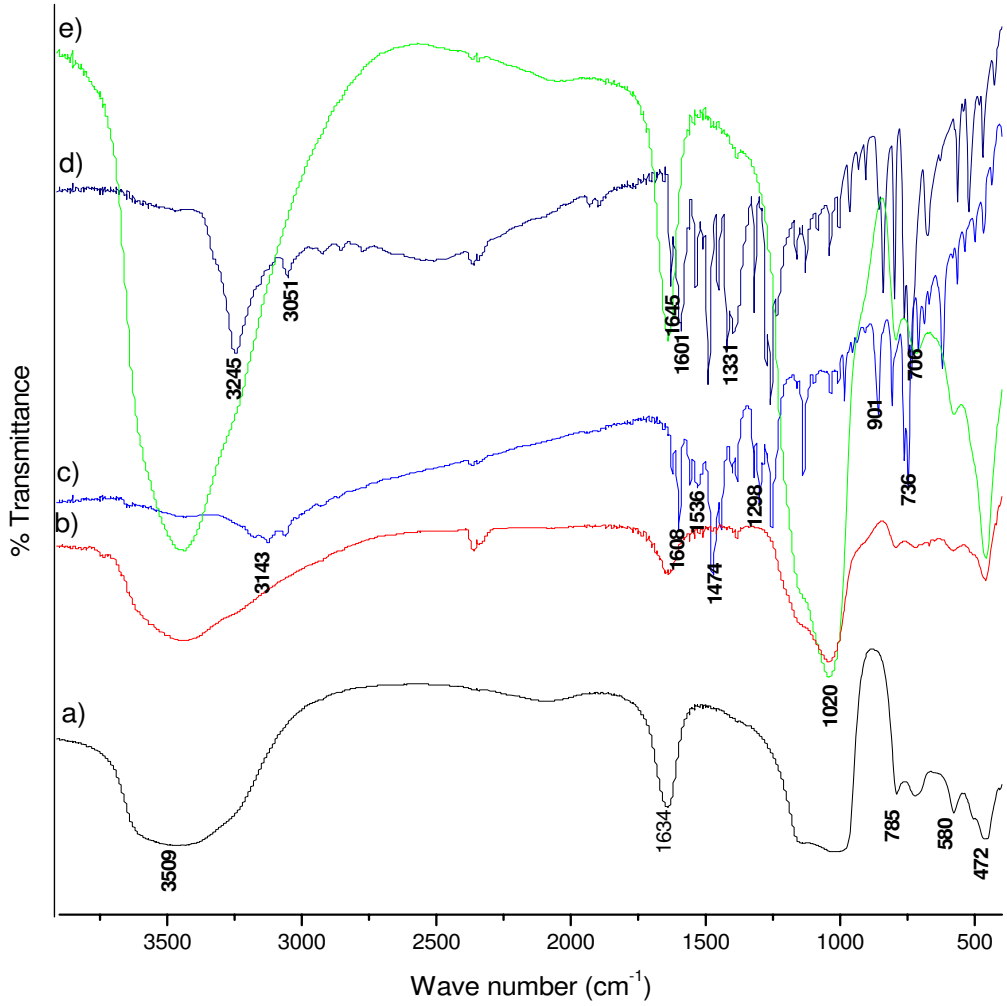

Figure 2: IR spectra of (a) Na-Y, (b) $Fe(opbmzl)_2$-Y, (c) $Fe(opbmzl)_2NO_3$, (d) ohpbmzl and (e) Fe-Y.

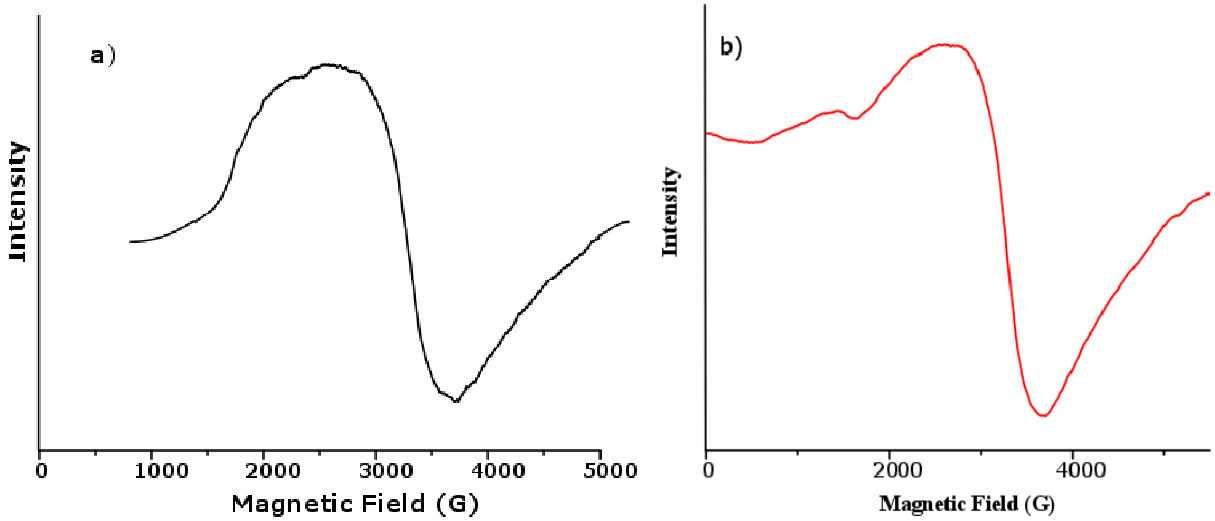

Figure 3: ESR spectra of a) Fe-Y and b) $Fe(opbmzl)_2Y$

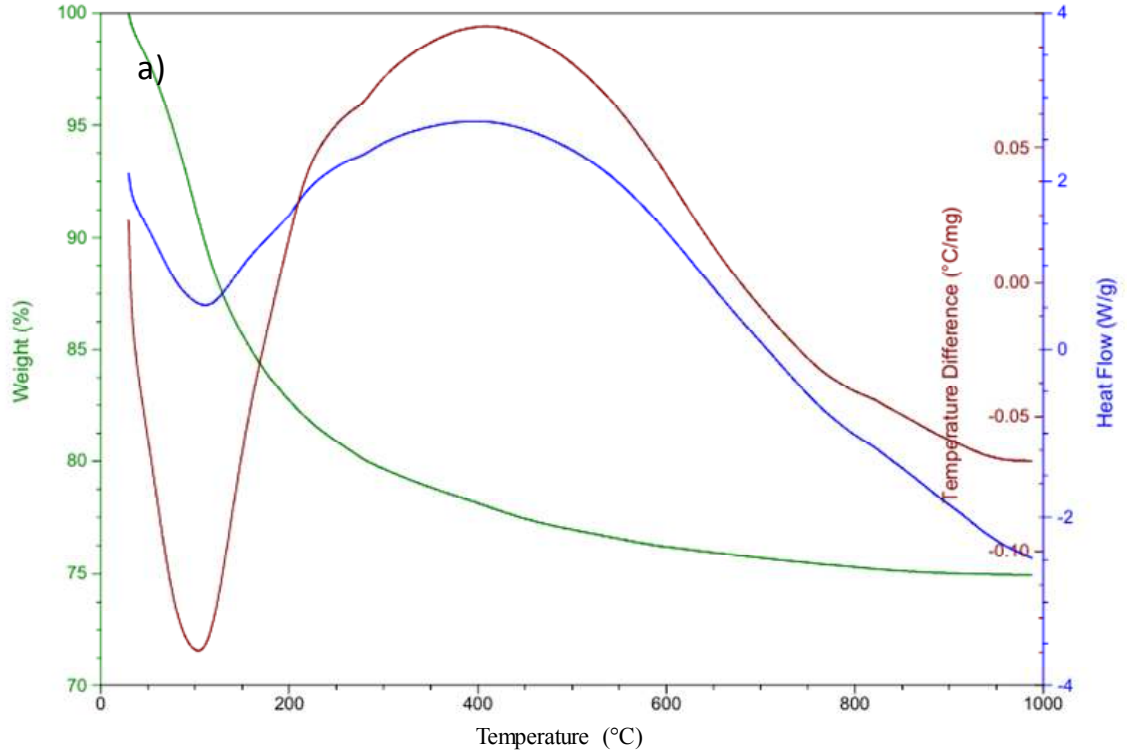

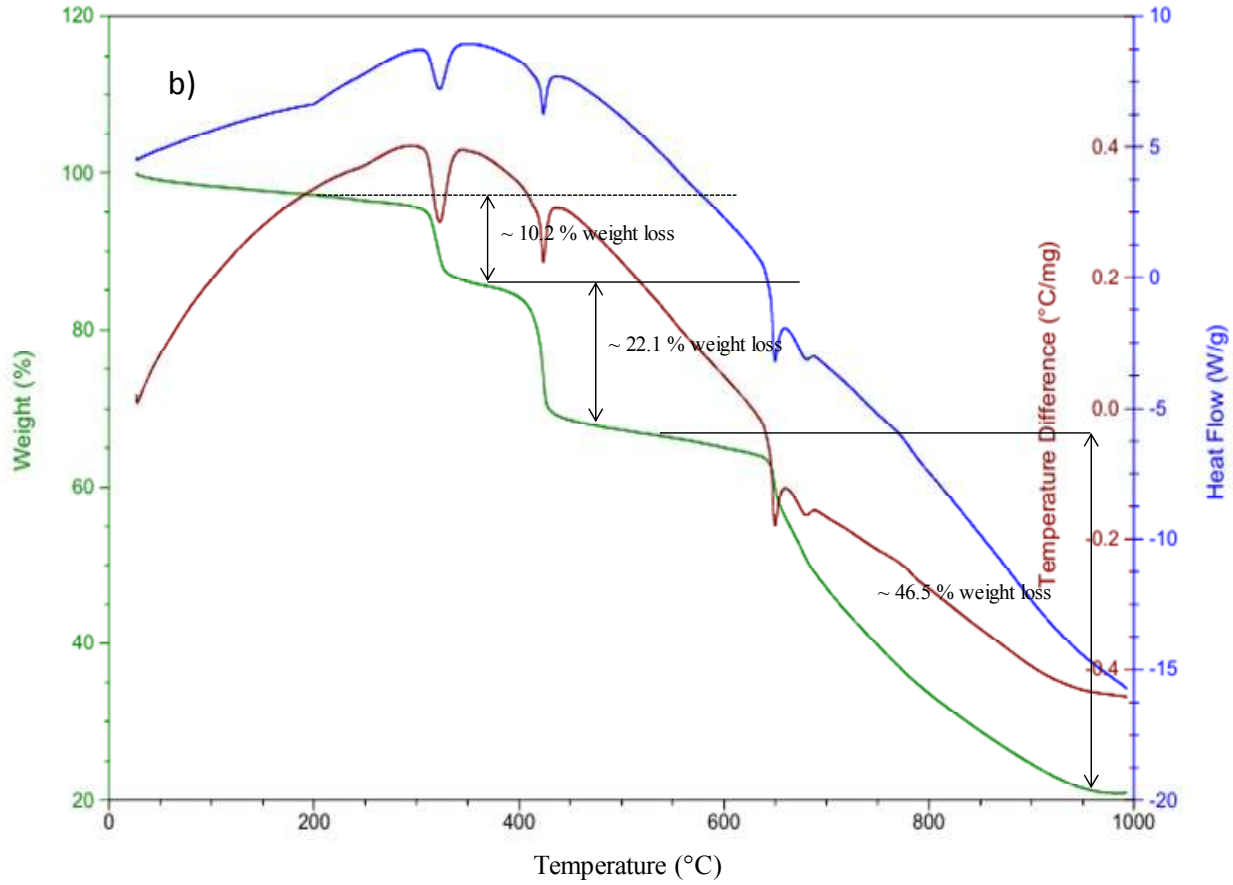

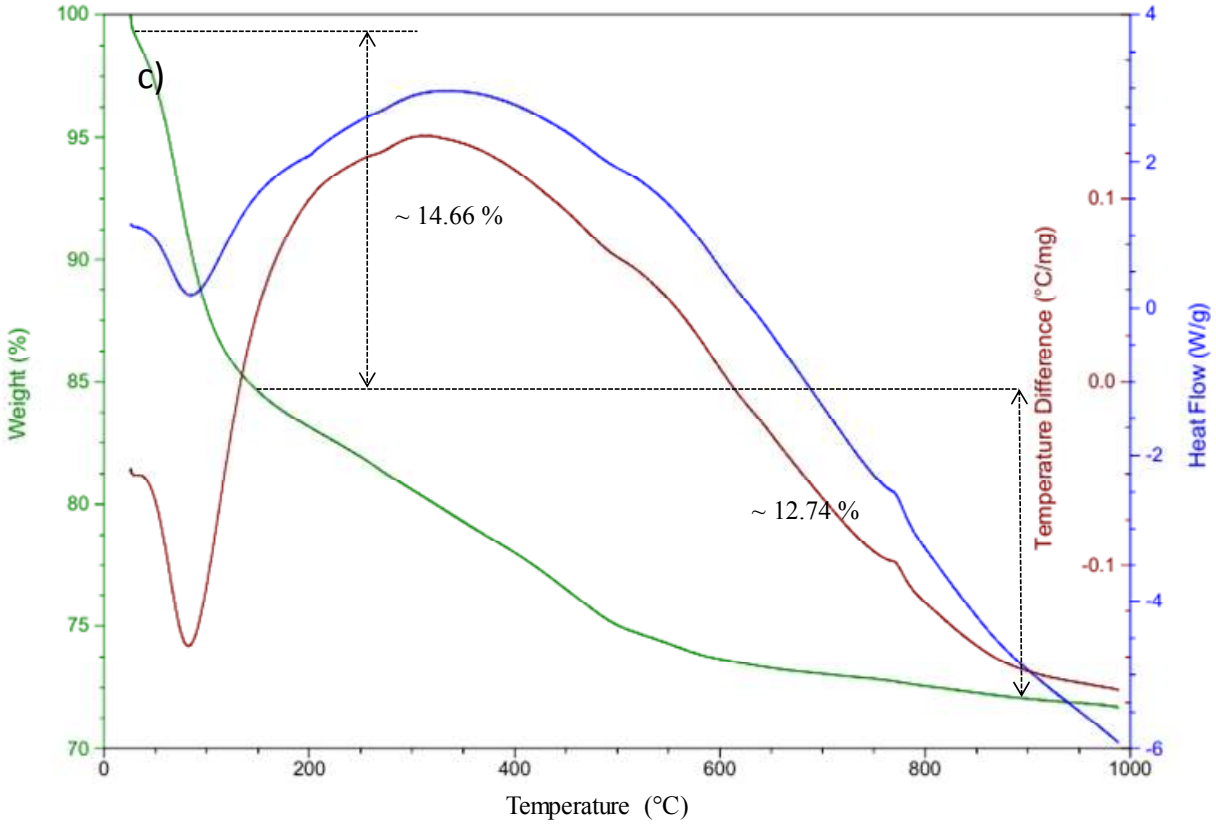

Figure 4: TGA decomposition profile of FeY, non-encapsulated and encapsulated complexes

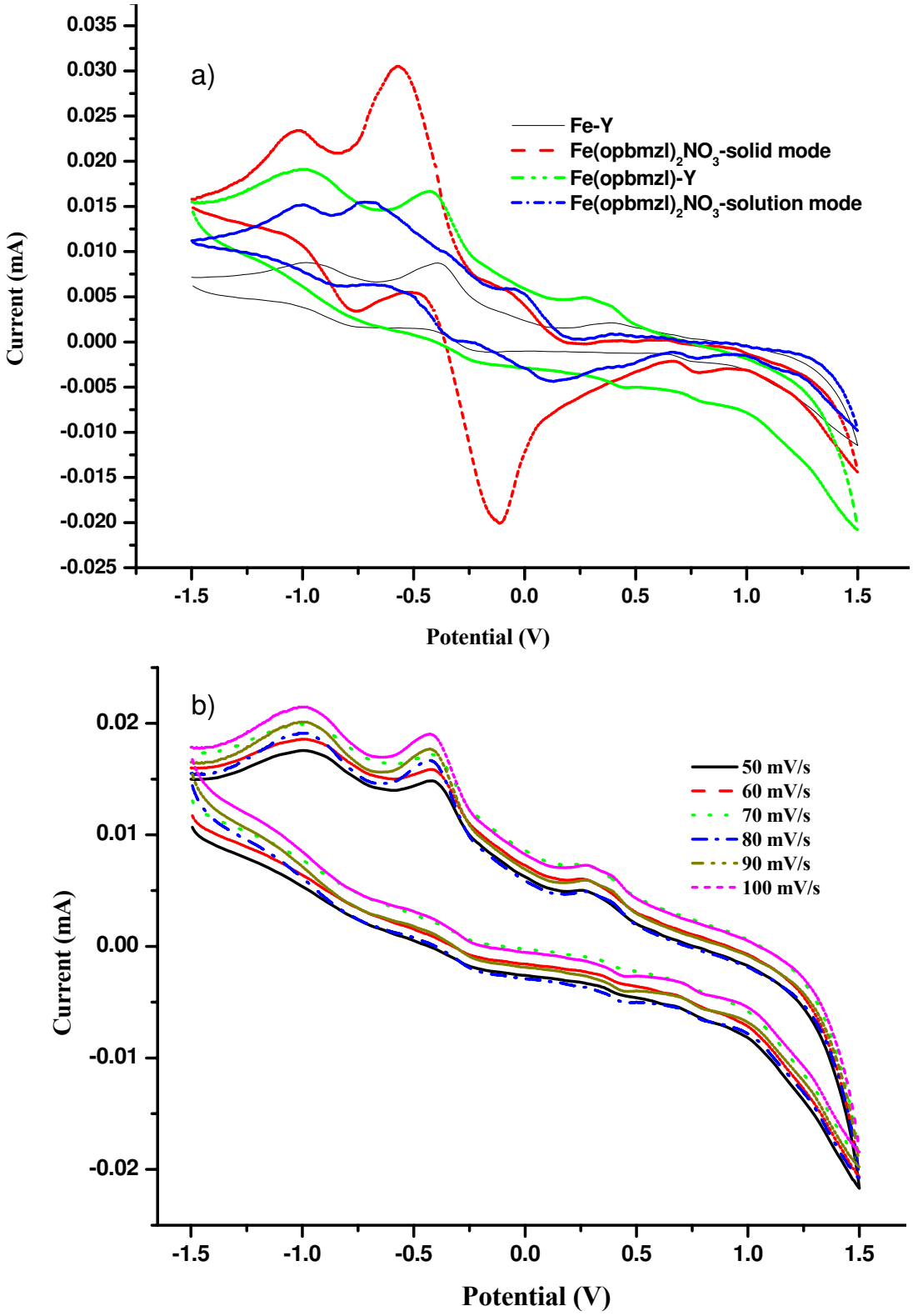

Figure 5: Cyclic voltammograms of a) Fe-Y, $Fe(opbmzl)_2NO_3$ in solution and solid mode and $Fe(opbmzl)_2Y$, b) $Fe(opbmzl)_2Y$ at different scan rates.

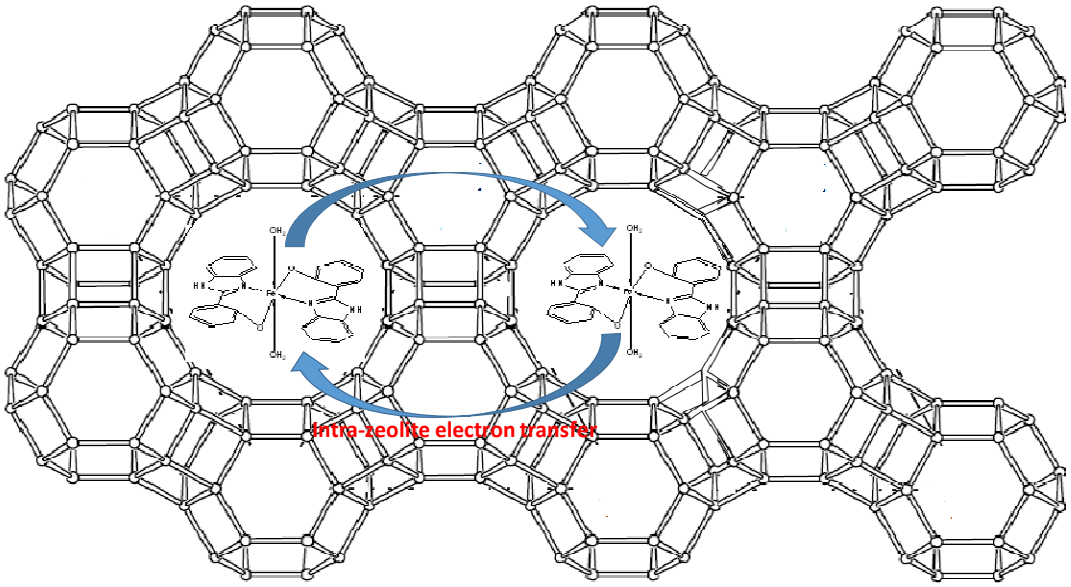

Figure 6: Graphical representation of electron transfer between encapsulated complexes in zeolite Y cavities.

Catalysts	Aniline conversion (%)	TON (10^2)	Product selectivity (%)	
			OBA	PBA
Fe(opbmzl) $_2$Y	84.4	2.3	4.4	95.6
Fe-Y	72.1	2	15.9	74.6
$Fe(opbmzl)_2NO_3$	76.5	2.1	6.8	87.9
NaY	12.9	0.3	65.4	34.6

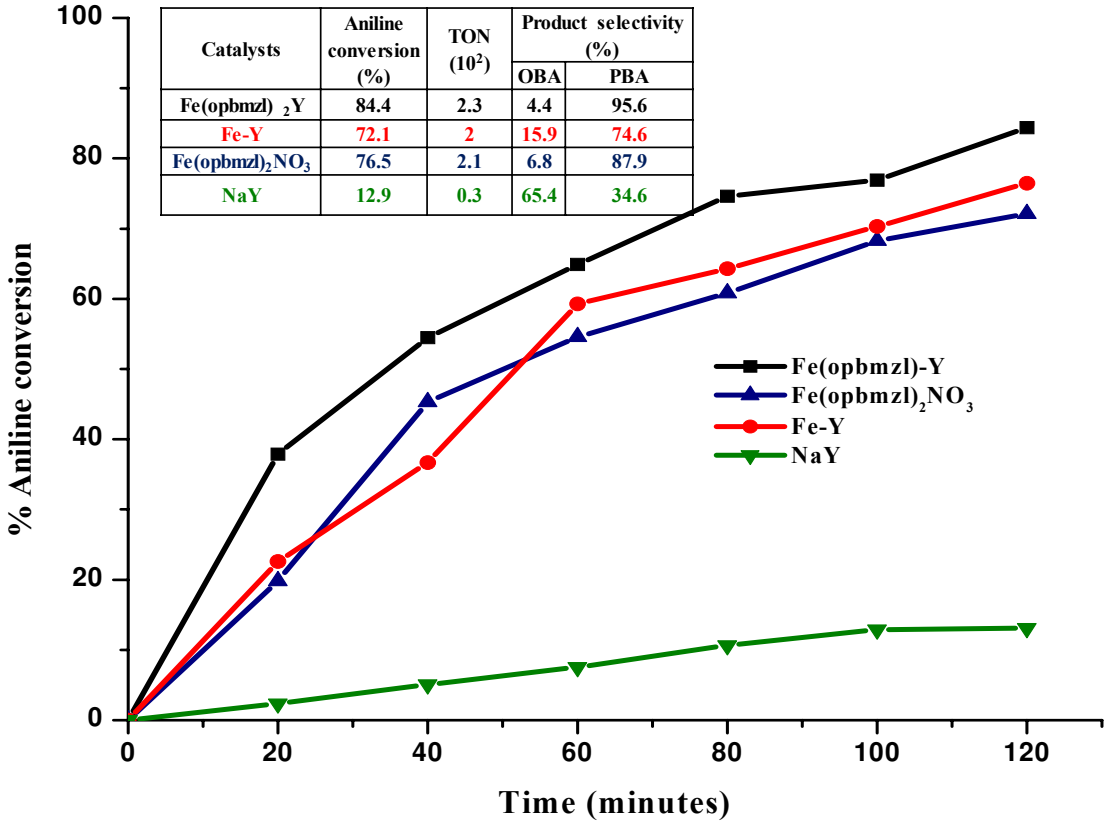

Figure 7: Reaction profile for oxidative bromination of aniline by the catalysts ($Fe(opbmzl)_2NO_3$, Fe-Y and $Fe(opbmzl)_2Y$ with respect to time.

Catalysts	Cyclohexane conversion (%)	TON (10^2)	Product selectivity (%)	
			OL	ONE
$Fe(opbmzl)_2Y$	**55.6**	**15.5**	**42.6**	**57.4**
Fe-Y	47.9	13.3	45.6	54.4
$Fe(opbmzl)_2NO_3$	**51.3**	**14.3**	**49.3**	**50.7**
NaY	4.9	1.2	64.3	35.7

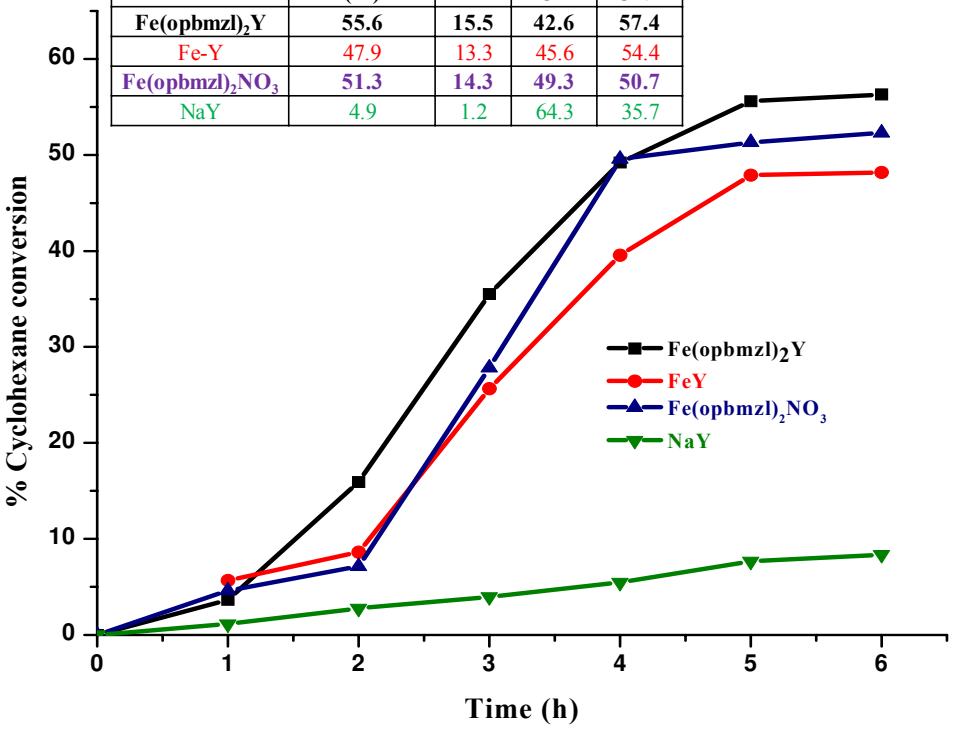

Figure 8: % Cyclohexane conversion for the catalysts NaY, $Fe(opbmzl)_2NO_3$, Fe-Y and $Fe(opbmzl)_2Y$.

Catalysts	Ethyl benzene conversion (%)	TON (10^2)	Product selectivity (%)		
			AP	BD	BA
Fe(opbmzl) $_2$Y	62.7	16.0	53.6	32.9	13.5
Fe-Y	51.2	12.7	39.6	36.9	23.5
$Fe(opbmzl)_2NO_3$	58.6	14.5	42.1	47.3	10.6
NaY	7.7	0.8	55.3	42.6	2.1

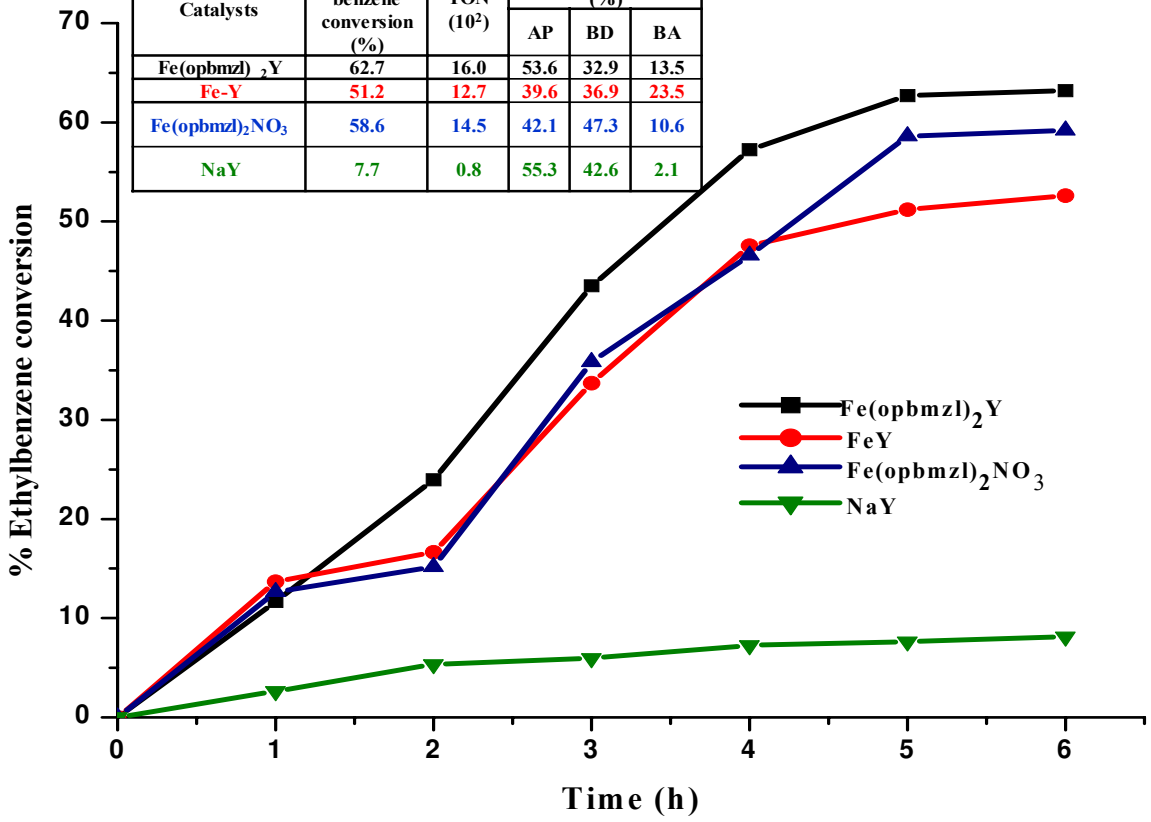

Figure 9: Effect of $Fe(opbmzl)_2NO_3$, Fe-Y and $Fe(opbmzl)_2Y$ on % ethylbenzene conversion

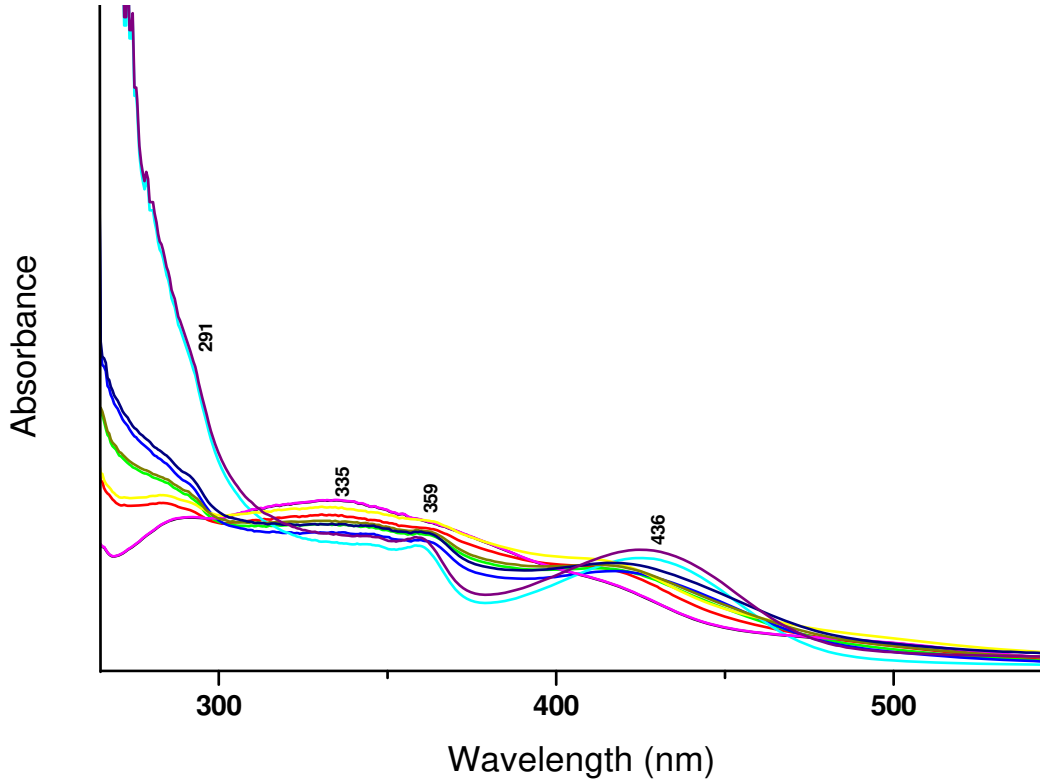

Figure 10: UV-vis absorption spectra for the titration of 10^{-3} M $Fe(opbmzl)_2NO_3$ in DMF with 10^{-3} M H_2O_2 solution in DMF.

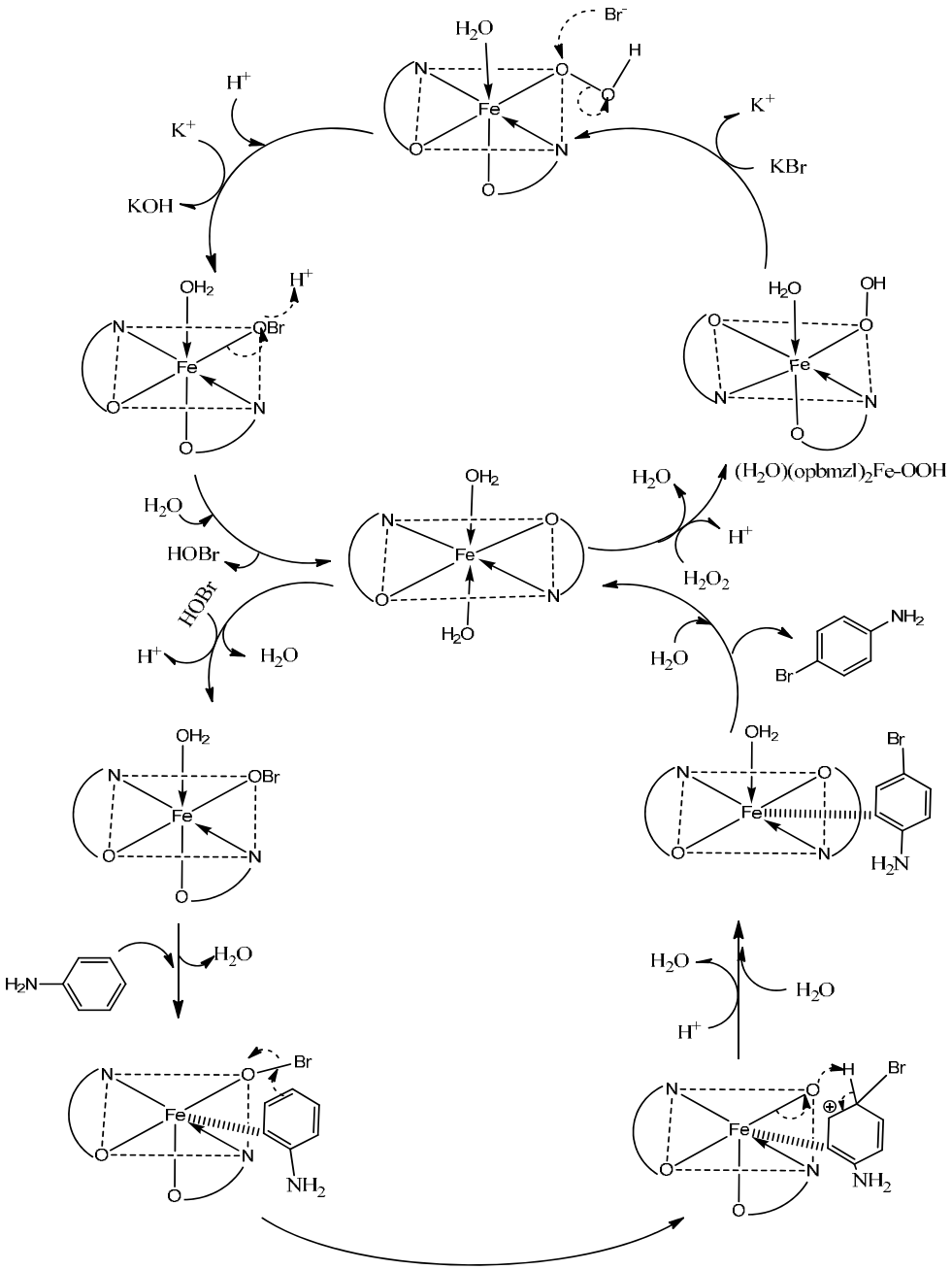

Scheme 2: Oxidative bromination of aniline by $Fe(opbmzl)_2$-Y

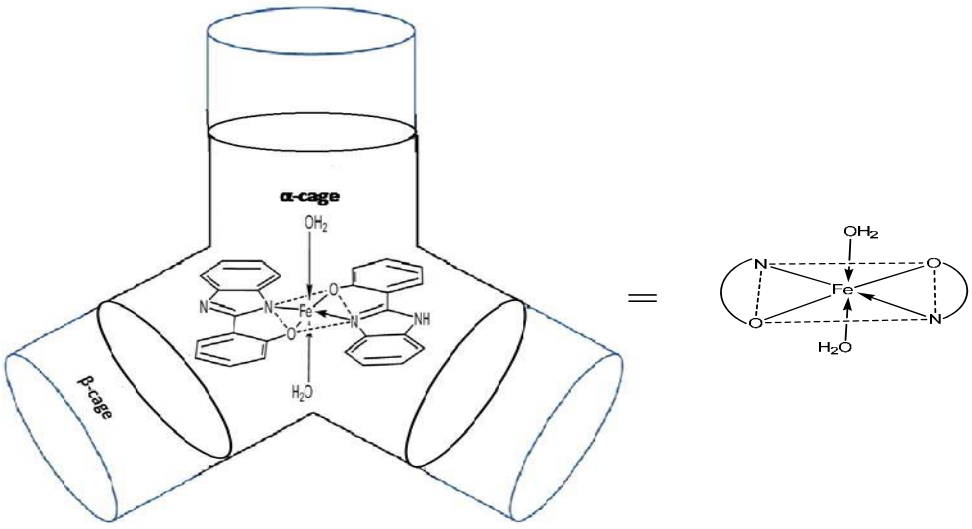

Zeolite-Y encapsulated Fe complex

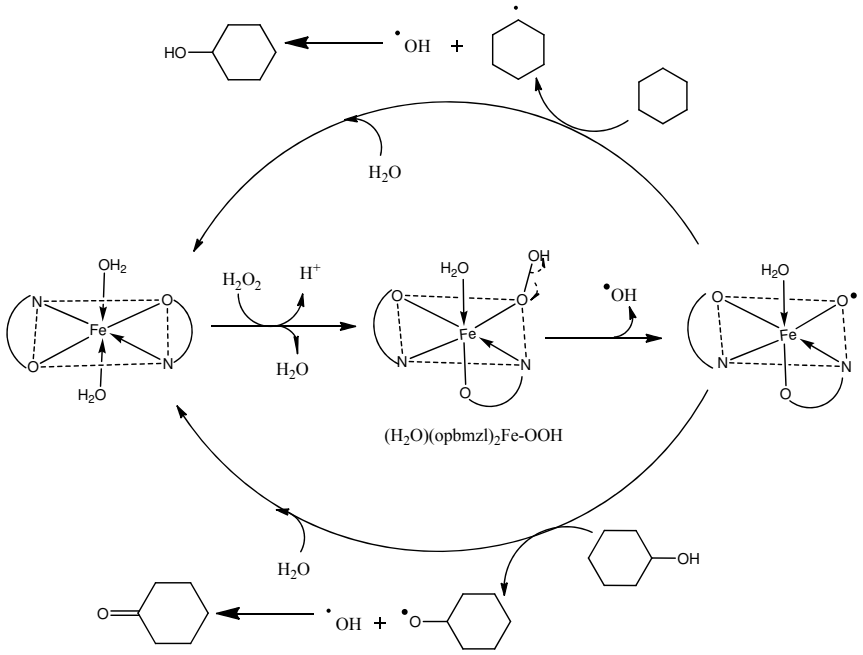

Scheme 3: Cyclohexane oxidation by Fe(opbmzl)$_2$-Y

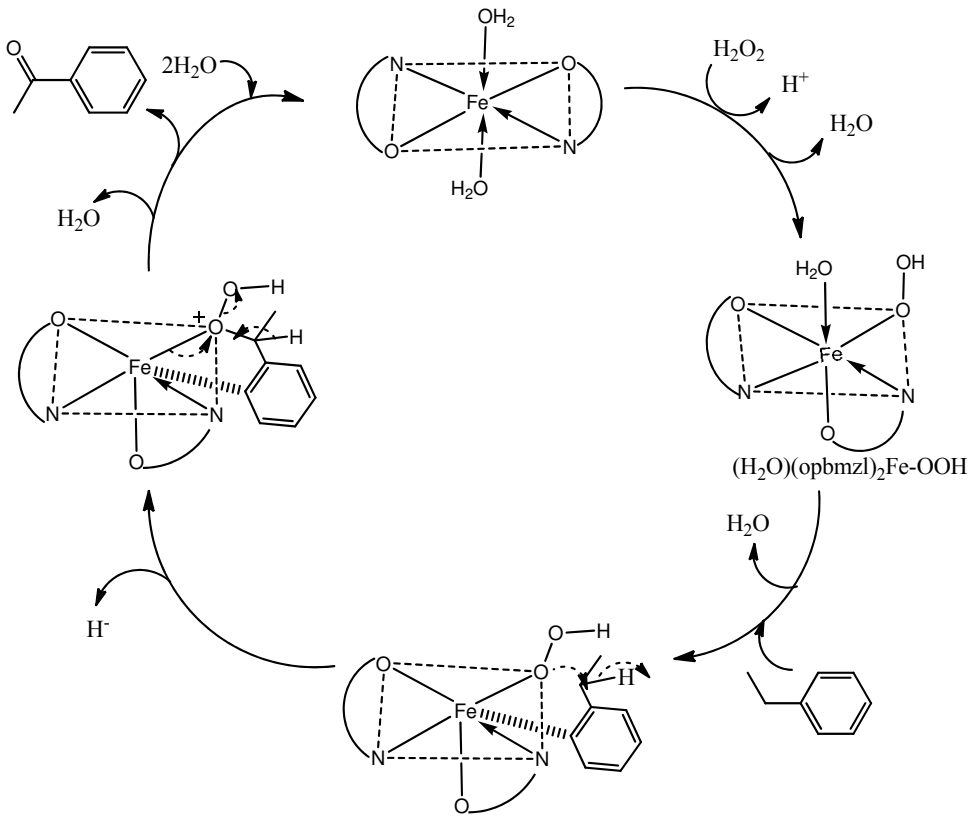

Scheme 4: Ethyl benzene oxidation by Fe(opbmzl)$_2$-Y

Table 1: Physical and textural properties of catalysts

Catalyst	Colour	Elemental analysis (%)			Textural Properties	
		C	N	Fe	Total pore volume (cc/g)	Surface area (m^2/g)
NaY	White	-	-	-	0.32	543.0
Fe-Y	Brown	-	-	1.7	0.26	350.5
$Fe(opbmzl)_2$-Y	Light Brown	1.71	0.42	0.45	0.24	334.8
$Fe(opbmzl)_2NO_3$	Wine red	57.68 (58.23)	12.62 (13.06)	9.48 (10.41)	-	-

* Calculated values in parenthesis

Table 2: UV-Vis/DRS spectral data (λ_{max} in nm) for the ligand, neat and encapsulated complexes

Sample	φ→φ*	π→π*	n→π*	Charge Transfer	d-d transitions
ohpbmzl	212	240	292	-----	-----
$Fe(opbmzl)_2NO_3$	219	233	290	331	474
$Fe(opbmzl)_2$-Y	204	248	295	366	505

Table 3: Oxidative bromination of various organic substrates catalyzed by $Fe(opbmzl)_2$-Y

Entry	Substrates	Conversion (%)	Product Selectivity (%)
1	Aniline	84.4	4-bromoaniline (95.6 %); 2-bromoaniline (4.4 %)
2	Phenol	72.3	4-bromophenol (100 %)
3	Anisole	72.0	4-bromoanisole (100.0 %)
4	Toluene	74.6	4-bromotoluene (93.0 %); 2-bromotoluene (7.0 %)
5	4-aminophenol	79.2	2-bromo-4-aminophenol (100 %))
6	Benzene	29.3	Bromobenzene (100 %))
7	Nitrobenzene	18.5	3-bromo-nitrobenzene (100 %)

Table 4: Recycling studies of $Fe(opbmzl)_2$-Y

Runs	Aniline conversion (%)	Product Selectivity (%)	
		OBA	PBA
I Cycle	84.4	4.4	95.6
II Cycle	83.1	12.5	85.6
III Cycle	79.3	14.6	80.3
IV Cycle	72.6	21.4	78.6
V Cycle	64.3	24.6	75.4
Runs	**Cyclohexane conversion (%)**	**Product Selectivity (%)**	
		OL	**ONE**
I Cycle	55.6	42.6	57.4
II Cycle	52.3	44.3	55.7
III Cycle	49.1	45.9	54.1
IV Cycle	45.6	49.1	50.9
V Cycle	38.8	51.4	48.6

Runs	Ethyl benzene conversion (%)	Product Selectivity (%)		
		AP	BD	BA
I Cycle	62.7	53.6	32.9	13.5
II Cycle	60.1	53.1	32.6	14.3
III Cycle	56.3	49.7	30.6	19.7
IV Cycle	51.1	49.3	28.3	22.4
V Cycle	47.3	47.1	25.6	27.3

Table 5: Comparison of the catalytic activity of $Fe(opbmzl)_2$-Y catalyst with other reported systems towards oxidative bromination

Sl. No	Catalyst	Reaction Conditions	Substrate	% conversion	Product Selectivity (%)	Reference
1	Polystyrene-divinylbenzene bound Fe(III) complex of Schiff base prepared by treating triethylenetetramine with salicylaldehyde	[Aniline] = 10 mmol; [KBr] = 20 mmol; [H_2SO_4] = 20 mmol; [H_2O_2] = 20 mmol; water (10 mL); [catalyst] = 50 mg; room temperature; Time = 2.5 h	Aniline	96.0	4-bromoaniline (85.0) 2-bromoaniline (15.0)	66
2	Fe_2O_3/zeolite	[Toulene] = 1 mL; [Br_2] = 0.5 mmol; [catalyst] = 10 mg; CH_2Cl_2; Temperature = 40°C, Time = 2 h;	Toulene	89.0	4-bromotoluene (51.0) 2-bromotoluene (38.0)	67
3	$FePO_4/SiO_2$	CH_4/ O_2 = 1.0; 40 wt.% HBr/H_2O = 2.0 ml/h; Temperature = 450 °C,	CH_4	17.1	CH_3Br (51.2), CH_2Br_2 (7.5)	68

4	$Fe(opbmzl)_2$-Y	[Aniline] = 10 mmol; [KBr] = 11 mmol; $[H_2O_2]$ = 25 mmol; Room temperature; Time = 3 h	Aniline	84.4	4-bromoaniline (95.6) 2-bromoaniline (4.4)	Present work
5	$Fe(opbmzl)_2$-Y	[Aniline] = 10 mmol; [KBr] = 11 mmol; $[H_2O_2]$ = 25 mmol; Room temperature; Time = 3 h	Toluene	74.6	4-bromotoluene (93.0) 2-bromotoluene (7.0)	Present work
5	$FePO_4$-SBA-15	$[CH_4]$ = 10 mL/min;40 wt.% HBr/H_2O 3.0 mL/h; $CH_4:O_2$ = 2:1 (v:v); O_2 = 5 mL/min; [catalyst] = 2.0 g; Temperature = 590 °C.	CH_4	12.1	CH_3Br (56.3), CH_2Br_2 (2.1)	69

Table 6: Comparison of the catalytic activity of $Fe(opbmzl)_2$-Y catalyst with other reported systems towards cyclohexane oxidation

Sl. No	Catalyst	Reaction Conditions	% conversion	Product Selectivity (%)	Reference
1	[Fe(III)(BPMP)Cl(l-O)Fe(III)Cl_3] {BBMP = (bis(2-pyr-idylmethyl)-1,4-piperazine)}	[H_2O_2] = 0.77 M; [catalyst] = 1.5 x 10^{-3} M in CH_3CN; Temperature = 40 °C.	19.2	Cyclohexanol (12.6) Cyclohexanone (6.6)	70
2	Fe(NC_3)Si-MCM-41{ NC_3.Si-MCM-41= 3-aminopropyltrimethoxysilane functionalized Si-MCM-41}	CH_3CN/Cyclohexane/H_2O_2 15/2/2 v/v/v; [catalyst] = 100 mg; Temperature = 70°C; Time =12 h.	30.0	Cyclohexanol (10.0) Cyclohexanone (20.0)	71
3	$[FeTSPc]_4$−{TSPc = tetrasulfophthalocyanine}	water/methanol (1:9); [cyclohexane] = 0.2 mol dm^{-3}; oxidant = THBP (0.8 mol dm^{-3}); [catalyst] = 6 × 10^{-6} mol dm⁻3; Time = 2h;	20.4	Cyclohexanol (21.0) Cyclohexanone (21.0) Others (58.0)	72
4	$Fe(opbmzl)_2$-Y	[cyclohexane] = 60 mmol;	55.6	Cyclohexanol (42.6)	Present

		$[H_2O_2]$= 150 mmol; [catalyst] = 0.120 g; CH_3CN (10 mL); Temperature = 70 ºC; Time = 6 h.		Cyclohexanone (57.4) Others (1.0)	work
5	Fe(III)-Schiff base complex in a Zn-Al LDH {Schiff base =2-amino nicotinic acid + salicylaldehyde}	[cyclohexane] = 18mmol, [catalyst] = 0.05 g; CH_3CN (10 mL); Temperature = 70 °C; Time = 8h,	45.5	Cyclohexanol (27.7) Cyclohexanone (72.3)	73
6.	Chitosan-supported iron(III) tetraphenylporphyrin	[catalyst] = 0.7843 g; Temperature = 145 °C; Time = 4.5h	10.48	Cyclohexanol (20.8) Cyclohexanone (79.2)	74
7.	$[Fe(VTCH)_2.2H_2O]$+-Y { VTCH=vanillinthiophene-2-carboxylichydrazone}	[cyclohexane] = 10mmol; $[H_2O_2]$ = 10mmol; [catalyst] = 60mg; CH_3CN (2mL); Temperature =	26.4	Cyclohexanol (42.2) Cyclohexanone (57.8)	75

		80°C; Time = 2h.			
8.	$[Fe(VFCH)_2.2H_2O]$ +-Y { VFCH=vanillinfuroic-2-carboxylichydrazone]	[cyclohexane] = 10mmol; $[H_2O_2]$ = 10mmol; [catalyst] = 60mg; CH_3CN (2mL); Temperature = 80 °C; Time = 2h.	11.6	Cyclohexanol (31.2) Cyclohexanone (68.8)	75
9.	Fe(III)TPPCl (Fe(III)tetraphenylporphyrin chloride) complex-Y	[cyclohexane] = 7.10 mmol; $[H_2O_2]$ = 12 mmol; [catalyst] = 0.21 g; CH_3CN (13 ml); Temperature = 80 °C; Time = 8 h	18.0	Cyclohexanol (35.0) Cyclohexanone (38.0) Others (27.0)	76

Table 7: Comparison of the catalytic activity of $Fe(opbmzl)_2$-Y catalyst with other reported systems towards ethylbenzene oxidation

Sl. No	Catalyst	Reaction Conditions	% conversion	Product Selectivity (%)	Reference
1	Fer-rocenecarboxaldehyde supported on SiO_2/Al_2O_3 supported aminopropyl (Si/Al APTMS ferrocene)	[ethylbenzene] = 9.0 mmol; [TBHP] = 9.0 mmol; [catalyst] = 5.0 mg, Temperature = 50 °C; Time = 24h	37.0	Acetophenone (87.0) Benzaldehyde(10.0) Others (3.0)	77
2	Fe_3O_4@SiO_2–NH_2@CS–Co(II)	[catalyst] = 0.3 g; H_2O_2 = HOAc; KBr, Temperature = 70°C, Time = 60 min	82.5	Acetophenone (80.4) Benzaldehyde(19.6)	78
3	Iron nanowire filled carbon nanotubes	[ethylbenzene] = 4.35 mol; 1.5 MPa O_2; [catalyst] = 100 mg; CH_3CN (30 mL),	36.8	Acetophenone (60.2) Benzaldehyde(21.1) Others (9.7)	79

4	$Fe(opbmzl)_2$-Y	Temperature = 155 °C, Time = 3 h, [ethylbenzene] = 40 mmol; H_2O_2 = 80 mmol; [catalyst] = 0.110 g; CH_3CN (10 mL); Temperature = 60 ºC; Time = 6 h.	62.7	Acetophenone (53.6) Benzaldehyde(32.9) Others (13.5)	Present work
5.	FeSHA/CPS (Fe-Salicylhydroxamate /chloromethylated polystyrene)	Temperature = 100 ºC; [catalyst] = 1.5 mmol/L; [tetraglycol] = 0.0463 mol/L; Time = 13 h; Lewis acid: 0.013 mol/L.	14.0	Ethylbenzenehydroperoxide 100.0	80